6.7 The Great Oxidation Event Transition

DC Catling, University of Washington, Seattle, WA, USA

6.7.1 Introduction

In Chapter 6.4, Farquhar et al. described geologic evidence for a significant increase in atmospheric O_2 levels at 2.45–2.32 Ga, while this chapter discusses why such a transition occurred. This chapter revolves around a basic principle of atmospheric chemistry, namely, that the concentration of an atmospheric gas is controlled by a kinetic competition between production and loss. This competition is described by fluxes, which, for a particular gas, are the rate of input to the atmosphere and the rate of chemical consumption. So, in its simplest formulation, there are only two options for explaining the Great Oxidation Event (GOE): either an increase of the O_2 source flux or a decrease of the O_2 sink flux created an imbalance. Most hypotheses in the literature argue that such changes in fluxes were probably gradual but reached a 'tipping point' when the O_2 source flux exceeded the consumption flux from reducing gases, allowing O_2 to rise to a new equilibrium level. The higher, post-GOE O_2 concentration was clearly determined by a new and different balance of fluxes. One can appreciate what controlled this new equilibrium with the naked eye. The ~2.3 Ga appearance of red beds, which are continental sediments stained by red-colored iron oxides, shows that atmospheric O_2 was lost in a quantitatively significant way to oxidative weathering after the GOE but not before. The oxidative weathering flux must have been very small prior to the GOE, given the absence of oxidation of continental surfaces in the Archean. To understand the change at the GOE, this chapter starts by describing the source and sink fluxes of O_2 as they are known today.

After describing general controls on O_2, this chapter discusses the other redox-sensitive gases in the atmosphere before and after the GOE. In the redox chemistry of the atmosphere, hydrogen-bearing reduced gases, such CH_4 and H_2, are the chemical adversaries of O_2. Through a series of photochemical reactions, there is a rapid mutual annihilation between O_2 and the reducing gases, akin to combustion in its net effect. In general, the redox chemistry of the pre-GOE atmosphere is dominated by methane and hydrogen molecules that spend an average of $\sim 10^4$ years in the atmosphere before being destroyed by reactions, whereas O_2 behaves as a trace gas with a short lifetime in the Archean atmosphere of less than a day (Pavlov et al., 2001). This situation in the Archean is the opposite of the modern atmosphere where methane and hydrogen are short-lived molecules with average lifetimes with respect to photochemical destruction of ~10 and ~2 years (e.g., Warneck, 2000), while O_2 has a lifetime of about 2 My with respect to geologic sinks (**Section 6.7.2.4**, in the following text). Possibly, reduced biogenic sulfur gases were also important constituents of the late Archean and pre-GOE Paleoproterozoic atmosphere. Models suggest that the GOE occurred when the rate of supply of O_2 to the atmosphere rose above the rate of supply of reduced gases to the atmosphere (Claire et al., 2006; Goldblatt et al., 2006; Holland, 2009). Because the atmosphere has a relatively small mass compared to the size of typical fluxes, the oxic transition probably happened relatively quickly from a geologic perspective. In photochemical simulations, the timescale is about 10^4 years (Claire, 2008), which is instantaneous in geologic time.

Finally, this chapter discusses the implications of the GOE for episodes of climate cooling and establishing an ozone layer. In detailed models, there is a decline in the supply of reducing gases prior to the GOE, which means that the methane concentration in the pre-GOE atmosphere should have fallen to a low level before O_2 rose to a substantial concentration (Zahnle et al., 2006). The collapse in the concentration of methane – a greenhouse gas, along with its photochemical

product, ethane – is generally consistent with low-latitude glaciation ('Snowball Earth') observed in the geologic record at ~2.4 Ga. In some geologic sections, such as the Huronian of Canada, the evidence for three glaciations appears between 2.45 and 2.22 Ga. Some biogeochemical models are able to produce oscillations in climate and atmospheric chemistry before establishing a permanent rise of O_2 (Claire et al., 2006). In these models, oxygenation events fail and the atmosphere reverts back to being weakly reducing before the Earth system attempts oxygenation again. Such behavior in models is entirely dependent upon how the output of biogenic, redox-sensitive gases is assumed to respond to the climate cooling associated with the GOE.

Ozone (O_3) is chemically derived from molecular oxygen. Once oxygenation was permanent, even with the relatively low levels of 0.2–2% O_2 by volume that existed in the middle Proterozoic, there was sufficient O_2 to establish a stratospheric ozone layer (Kasting and Donahue, 1980). The ozone layer would have protected the Earth's surface from harmful ultraviolet in the range 200–300 nm. A counterintuitive effect of the ozone layer was to decrease the net reaction rate in the troposphere between methane and oxygen by decreasing the input of ultraviolet photons. So, if methane fluxes were still relatively large from poorly oxygenated and euxinic marine waters in the Proterozoic, methane could have risen after the GOE to be a moderately significant greenhouse gas, although not to such large concentrations as in the Archean.

6.7.2 Controls on O_2 Levels

6.7.2.1 Hydrogen Escape to Space and Oxidation

There are both abiotic and biological net sources of O_2 for the atmosphere, but the latter source is dominant today by a factor of hundreds. Although the current abiotic source of O_2 is trivial, it is determined by the magnitude of the escape rate of hydrogen to space, which is worth discussing in some detail because this flux was almost certainly much bigger before the GOE. An anoxic atmosphere is relatively rich in hydrogen-bearing reducing gases (such as methane, CH_4, and hydrogen, H_2), which can drive relatively high rates of hydrogen escape. Hydrogen is the lightest gas, and planets the size of the Earth or smaller cannot hold on to hydrogen and undergo cumulative oxidation. Today, people observe the process of hydrogen escape on Saturn's moon, Titan, which has ~5% CH_4 in its lower atmosphere. They can also observe a halo of hydrogen around the modern Earth directly, some of which are escaping. The hydrogen atoms in the halo resonantly scatter Lyman-α (121.6 nm) ultraviolet radiation from the Sun and have been imaged by spacecraft (**Figure 1**). Today, the hydrogen escape flux is very small. But it helps to understand the hydrogen escape process in order to appreciate its potential oxidizing effect on Earth's early atmosphere when the flux of hydrogen escape was surely larger.

While hydrogen can escape to space, oxygen tends to remain behind because it is heavier. Indeed, it is universally accepted that the escape of hydrogen relative to heavier oxygen is responsible for the oxidized state of the atmospheres of Mars (Hunten, 1979), Venus (Watson et al., 1984; Zahnle and Kasting, 1986), and the extremely tenuous O_2-dominated atmospheres of several outer planet moons. The latter includes Ganymede (Hall et al., 1998) and Europa (Smyth and Marconi, 2006), which are satellites of Jupiter, and Rhea (Teolis et al., 2010) and Dione (Tokar et al., 2012), which are moons of Saturn. Some theories of oxygenation of the Earth give hydrogen escape a similarly important role in oxidizing

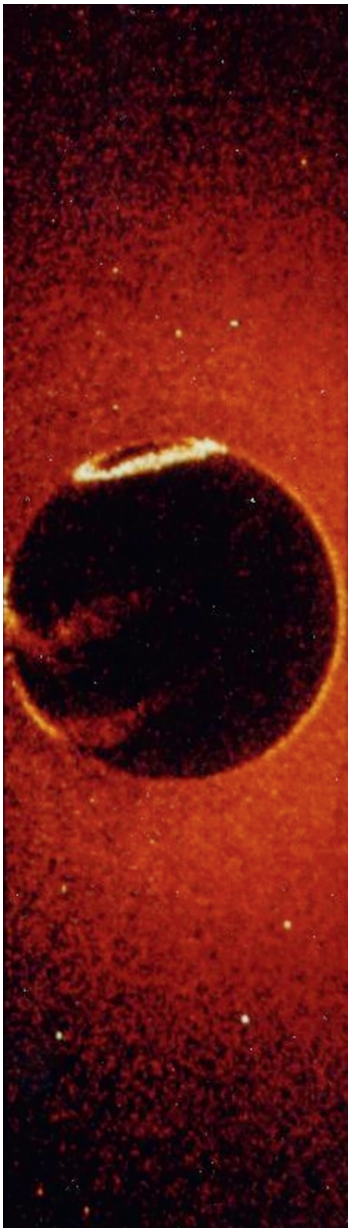

Figure 1 Hydrogen escape from the atmosphere is a directly observable phenomenon on the modern Earth. Above is an ultraviolet image of the Earth's dark hemisphere with the Sun behind it, taken from NASA's Dynamic Explorer 1 spacecraft at 19 700 km altitude above 13° N on 16 February 1982. The extended glow around the planet comes from hydrogen atoms that scatter Lyman-α radiation from the Sun. A northern auroral oval and equatorial glow are caused by emission from atomic oxygen and molecular nitrogen. Isolated points are stars that are bright in the ultraviolet (Courtesy of NASA).

the Earth and enabling the buildup of photosynthetic oxygen (Catling et al., 2001; Kasting et al., 1993). While hydrogen escape is the accepted explanation for the oxidation state of atmospheres of other planets and satellites, its role in the oxidation state of the Earth's atmosphere remains an area of debate, however.

The photolysis of gases in Earth's upper atmosphere and the escape of hydrogen to space provide an oxidation flux (Holland, 1978, p. 296). It is easy to see why. By the rules of redox chemistry, the hydrogen oxidation number 'decreases' from +1 in atmospheric compounds (such as H_2O vapor, CH_4, or H_2S) to 0 in H atoms that escape to space, which means that hydrogen gets reduced. Reduction is always accompanied by oxidation, so there must be an equivalent 'increase' in oxidation number, that is, oxidation, for other species on Earth when hydrogen escapes, irrespective of the details of the chemistry. While any particular redox reaction is redox-neutral, the oxidized and reduced components that are generated can be separated into different reservoirs. For the Earth as a whole, reduction of hydrogen to elemental form followed by hydrogen escape represents partitioning of the reduced component into space, leaving behind the oxidized component. The oxidation is irreversible because hydrogen that escapes into interplanetary space is lost forever from the Earth's gravitational field.

Oxygen-bearing gases can be photolyzed in the upper atmosphere to produce atomic oxygen (O) that can undergo atmospheric reactions to make abiotic molecular oxygen, O_2. For example, H_2O and CO_2 are photolyzed as follows:

$$\begin{aligned} H_2O + h\nu &\rightarrow H + OH \\ CO_2 + h\nu &\rightarrow CO + O \end{aligned} \qquad [1]$$

Molecular oxygen, O_2, can be produced from the O atoms and hydroxyl (OH) radicals made from the reactions in eqn [1] as follows:

$$O + OH \rightarrow O_2 + H \qquad [2]$$

If hydrogen does not escape, O_2 is lost in catalytic cycles and water vapor is reformed as follows:

$$\begin{aligned} H_2O + h\nu &\rightarrow H + OH \\ H + O_2 + M &\rightarrow HO_2 + M \\ 3 \times \ldots H_2 + OH &\rightarrow H_2O + H \\ H + HO_2 &\rightarrow 2OH \\ H + H + M &\rightarrow H_2 + M \\ \hline 2H_2 + O_2 &\rightarrow 2H_2O \end{aligned} \qquad [3]$$

Alternatively, if hydrogen escapes to space, the products of photolysis cannot recombine and O_2 is leftover. Thus, it is the escape of hydrogen to space that is essential for making O_2. So a net oxidation flux from photochemistry is always determined by the escape flux of hydrogen.

Under a wide variety of circumstances, which apply to the Archean atmosphere as well as the present one, the escape of hydrogen to space is constrained by two 'bottlenecks' in the atmosphere, shown schematically in Figure 2 (following Hunten, 1990). The first bottleneck is the 'tropopause cold trap,' which limits the transport of hydrogen within water vapor to the upper atmosphere. The Earth's tropopause is the minimum temperature in the vertical temperature profile that occurs at the top of the Earth's troposphere. The troposphere

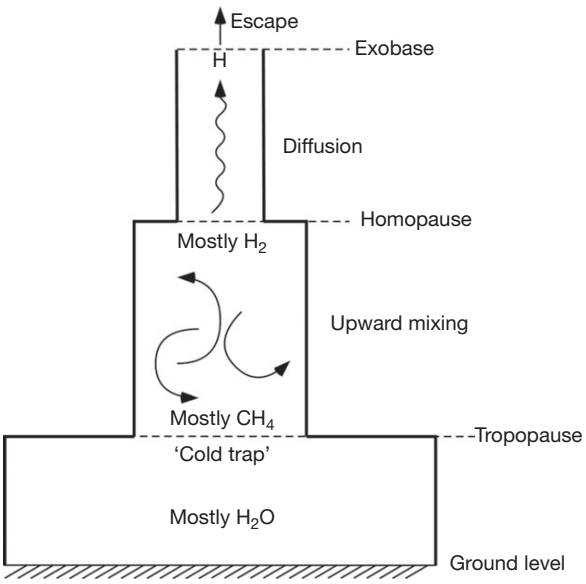

Figure 2 A conceptual diagram showing 'bottlenecks' for hydrogen escape from the Earth's atmosphere. At the tropopause, most water vapor condenses and the dominant form of hydrogen just above the tropopause is in the form of methane, even on the modern Earth. Hydrogen in all its forms is mixed up through the stratosphere and mesosphere, but its transport is then rate-limited by diffusion through the thermosphere to the boundary with space, the exobase. By the time the hydrogen gets to the exobase, it is mostly in atomic form.

extends vertically from the Earth's surface to ~17 km at the equator or to lower altitudes at other latitudes. The tropopause acts as a brake on vertical transport in the atmosphere because the energy balance in the atmosphere changes from convection-dominated in the troposphere to radiation-dominated just below the tropopause. Convection is sufficiently strong in the warm tropics to lift water vapor up and through the tropical tropopause. However, at the tropical tropopause, water vapor freezes into ice particles (hence the name 'cold trap') so that very little water vapor enters the lower stratosphere. Consequently, the lower stratosphere is extremely arid with only ~3 ppmv H_2O. Other hydrogen-bearing constituents, such as methane (CH_4) and diatomic hydrogen (H_2), have condensation temperatures that are far too low to be cold-trapped in Earth's atmosphere, so these gases mix through the tropopause and their abundance in the lower stratosphere is about the same as in the troposphere. Ultimately, stratospheric water vapor is broken down at high altitudes through photochemical reactions. The resulting hydrogen, along with the hydrogen derived from methane and molecular hydrogen, is transported upward and mixed by eddies through the stratosphere and mesosphere.

The second bottleneck for hydrogen escape occurs when the upwardly mixed hydrogen reaches the 'homopause,' around 100 km altitude. The homopause is the level above which gases separate out diffusively with altitude according to their mass. Consequently, the air above the homopause becomes increasingly enriched in molecules or atoms that have lower mass than the average. Hydrogen, being lighter than all other gases, rises buoyantly through the background air by molecular diffusion. Fortunately, the diffusion rate is readily calculable

and sets a 'diffusion-limited escape rate,' which is the maximum rate that hydrogen can be transported upward by diffusion and escape (Hunten, 1973). Essentially, diffusion acts as another brake on the upward transport of hydrogen to space. Hydrogen is mostly broken down into atomic form and escapes efficiently from the 'exobase,' which is the level in the atmosphere, typically around 400–500 km altitude, above which collisions between atoms and molecules are so infrequent that they can be neglected. This lack of collisions means that there is nothing to prevent hydrogen atoms with upward-directed velocities exceeding the escape velocity being lost permanently to interplanetary space from the exobase. So while the tropopause cold trap modulates the amount of hydrogen that can reach the upper atmosphere and escape, molecular diffusion above the homopause sets the maximum rate that hydrogen can escape once it gets to ~100 km altitude. Hence, the cold trap and diffusion are said to be the two 'bottlenecks' on hydrogen escape (Hunten, 1990).

The theory of diffusion-limited escape gives a hydrogen escape rate, Φ_H, as follows (Walker, 1977):

$$\Phi_H \cong \frac{b_H f_T}{H} = (\text{constant}) f_T \approx (2.5 \times 10^{13}) f_T \quad (\text{atoms cm}^{-2}\ \text{s}^{-1}) \qquad [4]$$

Here, b_H is a binary diffusion parameter for hydrogen through air, where one uses an average for H_2 and H, weighted by their probable mixing ratios at the homopause in order to obtain the constant in the second expression. The variable H is the atmospheric scale height for the background gas, given by $H = kT/(mg)$, where k is Boltzmann's constant (1.38×10^{-23} J K^{-1}), T is the mean atmospheric temperature at the homopause, m is mean molecular mass, and g is gravitational acceleration. The remaining term, f_T, is the total hydrogen mixing ratio at the homopause, given by the sum of the mixing ratios of hydrogen in all of its chemical forms, weighted by the number of hydrogen atoms each species contains, that is,

$$f_T = f_H + 2f_{H_2} + 2f_{H_2O} + 4f_{CH_4} + \cdots \qquad [5]$$

Here, f_H is the mixing ratio of H atoms, f_{H_2} is the mixing ratio of H_2 molecules, f_{H_2O} is the mixing ratio of water vapor, and CH_4 is the mixing ratio of methane. Because the total hydrogen mixing ratio is approximately conserved with altitude from the lower stratosphere to the homopause (as expected from theory and observation; Harries et al., 1996), one can evaluate eqn [5] with values that are well known from measurements in the lower stratosphere.

The current hydrogen escape rate and the associated oxidation rate can easily be calculated using the theory earlier. In today's lower stratosphere, the concentrations of hydrogen-bearing gases are 1.8 ppmv CH_4, ~3 ppmv H_2O, and 0.55 ppmv H_2. Using eqn [5], the total mixing ratio of hydrogen, f_T, is 14.3×10^{-6} ($= [2(0.55) + 4(1.8) + 2(3)] \times 10^{-6}$). Consequently, the hydrogen escape rate from eqn [4] is 3.6×10^8 atoms cm^{-2} s^{-1}. Given that the area of the Earth is 5.1×10^{18} cm^2, the escape rate for the whole Earth is $(3.6 \times 10^8$ atoms cm^{-2} s$^{-1}) \times (5.1 \times 10^{18}$ cm$^2) = 1.8 \times 10^{27}$ atoms s^{-1} = 3 kg H s^{-1} = 9.3×10^{10} mol H atoms year^{-1} = 93 000 tons of H year^{-1}. By redox balance, the escape of four moles of hydrogen atoms is equivalent to an oxidation flux of one mole of oxygen (which one can deduce through the schematic redox balance of $4H + O_2 = 2H_2O$). Consequently, the net oxidation flux for the whole Earth from today's escape of hydrogen to space is equivalent to 2.3×10^{10} mol O_2 year^{-1}. This flux is negligible compared to the biological flux of O_2 (~10^{13} mole O_2 year^{-1}), which is discussed in the succeeding text. However, the hydrogen escape flux must inevitably have been larger in the pre-GOE atmosphere, which was redox-dominated by hydrogen-bearing species. A higher total mixing ratio of hydrogen in all its forms leads to a larger total hydrogen mixing ratio, f_T, in eqn [5]. Consequently, there is a proportionately greater hydrogen escape rate, Φ_H. For example, the anoxic Archean atmosphere probably had ~10^3 ppmv CH_4 (Kasting et al., 2001). In that case, the oxidation flux of hydrogen escape from eqns [4] and [5] was significant and ~7×10^{12} mol O_2 year^{-1}.

6.7.2.2 The Net Source Flux of Oxygen

Molecular oxygen in the modern atmosphere is produced almost entirely as the waste product of 'oxygenic photosynthesis' – the type of photosynthesis in which green plants, algae, and cyanobacteria use sunlight to split water molecules. More generally, photosynthesis is the biological process by which carbon dioxide is chemically reduced with hydrogen with an overall scheme as follows:

$$2H_2A + CO_2 + h\nu \rightarrow CH_2O + H_2O + 2A\ (\text{or } A_2) \qquad [6]$$

Here, A designates an atom that varies depending on the type of photosynthesis, and 'CH_2O' represents organic matter as carbohydrate. It is generally thought that 'anoxygenic photosynthesis' (which does not release O_2) was ancestral to oxygenic photosynthesis because it is chemically simpler and because the genetics of microbes implies such a lineage (Xiong, 2006). The suspected evolutionary sequence is that the first photosynthetic microbes used H_2 (eqn [6] with no 'A'). These were probably followed by microbes that used hydrogen sulfide, where 'H_2A' as H_2S in eqn [6]:

$$2H_2S + CO_2 + h\nu \rightarrow CH_2O + H_2O + 2S \qquad [7]$$

Photosynthesis that uses ferrous iron also evolved. Iron photosynthesis does not quite fit the generic scheme earlier but can be written

$$4Fe^{2+} + CO_2 + 11H_2O + h\nu \rightarrow CH_2O + 4Fe(OH)_3 + 8H^+ \qquad [8]$$

In oxygenic photosynthesis, water is split. So, in eqn [6], 'H_2A' is H_2O and the waste product is O_2 derived from the O atoms in H_2O. The equation representing oxygenic photosynthesis and the reverse processes of respiration or oxidative decay can be simplified to

$$H_2O + CO_2 + \text{energy} \underset{\text{respiration, decay}}{\overset{\text{photosynthesis}}{\rightleftharpoons}} CH_2O + O_2 \qquad [9]$$

In this equation, a mole of organic matter accompanies every mole of O_2 generated by photosynthesis. But within ~10^2 years, almost all the O_2 produced in photosynthesis is used up in oxidizing organic matter back to carbon dioxide in respiration or decay. Consequently, when one considers geologic timescales of millions of years, one can ignore this fast, gross cycle of zero sum photosynthesis and focus on the net

production. In net production, about 0.1–0.2% of the organic carbon is buried, mostly in deltaic sediments of continental shelves (Berner, 1982), where it escapes the fate of being oxidized. The burial flux of organic carbon is estimated to be 10.0 ± 3.3 Tmol C year^{-1} today (Holland, 2002), which, by the 1:1 stoichiometry of eqn [9], provides 10.0 ± 3.3 Tmol O_2 year^{-1} (here and elsewhere, 1 Tmol $= 10^{12}$ mol). Berner (2004), p. 42, gives a somewhat lower estimate of 5.3 Tmol C year^{-1} for the organic burial flux. For consistency with other estimates, we will follow Holland's numbers.

In the modern O_2 balance, the burial of other reductants can also contribute to O_2 production, of which sulfur and iron are the most significant (Figure 3). At the seafloor, bacteria use organic carbon to make pyrite (FeS_2) from the reduction of seawater sulfate that diffuses into the sediments. When the pyrite is subsequently buried, it effectively removes the reduced partner of O_2 from being oxidized and provides a source of O_2. Pyrite generation and burial can be written as follows (Berner, 2004):

$$\begin{array}{lrl} \text{Photosynthesis :} & 15H_2O + 15CO_2 & = 15CH_2O + 15O_2 \\ \text{Sulfate reduction :} & 15CH_2O + 2Fe_2O_3 + 16H^+ + 8SO_4^{2-} & = 4FeS_2 + 23H_2O + 15CO_2 \\ \text{Net :} & 15H_2O + 15CO_2 & = 15CH_2O + 15O_2 \end{array} \quad [10]$$

Holland (2002) estimates that the pyrite burial flux contributes 7.8 ± 4.0 Tmol O_2 year^{-1}. Other minerals that are important for the redox balance include sulfates, which can be buried as evaporite minerals on continents, and ferrous iron. Their fluxes can be estimated from examining the quantity of various redox-sensitive minerals in average sedimentary rocks, as shown in Table 1.

6.7.2.3 The Oxygen Sink Fluxes

In recent geologic history, the flux of O_2 from the sources shown in Table 1 must be approximately balanced by sink fluxes so that the O_2 level remains relatively stable. The persistence of advanced animals that rely on high O_2 concentrations for the past several hundred million years suggests that there were no wildly fluctuating O_2 levels during this period. Figure 3 depicts the various sink fluxes that remove O_2 from the atmosphere, which we now quantify.

The process of continental oxidative weathering occurs when O_2 dissolved in rainwater or rivers reacts with reduced minerals on the continents, such as exposed organic carbon, ferrous iron (Fe^{2+}) minerals, and sulfides. Essentially, continental weathering reverses the chemical equations that liberate O_2 shown in Table 1. Examining average continental rock allows estimates

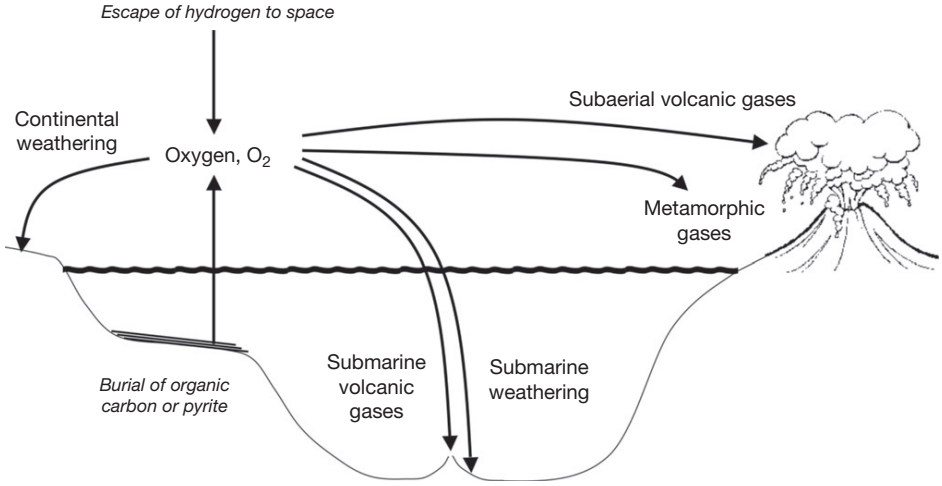

Figure 3 Schematic diagram showing the long-term sources and sinks of oxygen fluxes.

Table 1 The source flux of O_2 on modern geologic timescales (sedimentary sources following Holland (2002))

Process		*Stoichiometry*	*O_2 gain (Tmol year^{-1})*
Hydrogen escape		$2H_2O \rightarrow 4H(\uparrow\text{space}) + O_2$	0.02
	Wt% in new sediments		
Carbon burial	0.6 ± 0.1	$CO_2 \rightarrow C + O_2$	10 ± 3.3
Pyrite burial	0.6 ± 0.2	$Fe(OH)_3 + 2H_2SO_4 \rightarrow FeS_2 + 15/2SO_2 + 7/2H_2O$	7.0 ± 3.6
Pyrite burial	0.2 ± 0.1	$FeO + 2SO_2 \rightarrow FeS_2 + 5/2O_2$	0.8 ± 0.4
Sulfate burial	0.3 ± 0.1	$SO_2 + 1/2O_2 + H_2O \rightarrow H_2SO_4$	$-(0.3 \pm 0.1)$
Fe^{2+} burial	1.5 ± 0.6	$1/2Fe_2O_3 \rightarrow FeO + 1/4O_2$	0.9 ± 0.4
		Total rate of oxygen production =	18.4 ± 7.8

for the rate of continental weathering of various minerals to be made. The estimates in Table 2 sum to a loss of 15.5 ± 6.7 Tmol O_2 year^{-1} during continental weathering.

Other sinks of O_2 arise from reactions with various reductants that include gases, such as H_2, CO, CH_4, H_2S, and SO_2, released from high-temperature subaerial volcanism (where rocks melt) and metamorphism (where the rocks are heated but do not melt), seafloor minerals encountered by O_2 dissolved in percolating seawater, and gases and dissolved minerals released from hydrothermal vents into the oceans. Table 2 lists various estimates from the literature for these sink fluxes.

Within the rather large uncertainty, the total source flux of 18.4 ± 7.8 Tmol O_2 year^{-1} from Table 1 agrees with the total sink flux of 22.1 ± 8.4 Tmol O_2 year^{-1} given in Table 2. The sink fluxes in Table 2 imply that about 70% of the O_2 in the atmosphere is eventually removed by oxidative weathering, while the remaining 30% is lost to metamorphism, subaerial volcanism, seafloor weathering, and submarine volcanism, going in order from the largest to smallest sink.

6.7.2.4 General Principles of Oxygen Change

For a steady concentration of O_2 in the atmosphere–ocean system, the O_2 source flux, $F_{O_2\text{source}}$, must be equal to the O_2 sink flux, $F_{O_2\text{sink}}$. Oxygen levels will obviously increase if the source flux exceeds the sink flux. For specificity, it is advantageous to consider O_2 changes mathematically, in terms of a flux balance equation. If one denotes the reservoir of O_2 in the atmosphere–ocean system as R_{O_2}, it will change with time, t, as follows:

$$\begin{aligned}\frac{d(R_{O_2})}{dt} &= F_{O_2\text{source}} - F_{O_2\text{sink}} \\ &= F_{O_2\text{source}} - (F_{\text{volcanic}} + F_{\text{metamorphic}} + F_{\text{weathering}})\end{aligned} \quad [11]$$

Here, the O_2 source flux arises from the relatively limited number of processes shown in Table 1, principally the burial of organic carbon. In contrast, the O_2 sink fluxes comprise a very large number of chemical reactions shown in Table 2. In the second line of eqn [11], the sink fluxes are broken up into three types: F_{volcanic}, which is the flux of O_2 that reacts with reductants from subaerial and submarine volcanism;

Table 2 Modern long-term sink fluxes for O_2

Loss process		*Stoichiometry*	*O_2 loss (Tmol year^{-1})*	*References*
Continental weathering				
	Wt% in average rock undergoing weathering			
Carbon weathering	0.45 ± 0.1	$C + O_2 \rightarrow CO_2$	7.5 ± 2.5	Holland (2002)
Sulfide weathering	0.6 ± 0.2	$FeS_2 + 15/2SO_2 + 7/2H_2O \rightarrow Fe(OH)_3 + 2H_2SO_4$	7.0 ± 3.6	Holland (2002)
Fe^{2+} weathering	1.5 ± 0.6	$FeO + 1/4O_2 \rightarrow 1/2Fe_2O_3$	1.0 ± 0.6	Holland (2002)
Subtotal for continental oxidative weathering flux = 15.5 ± 6.7				
Surface volcanism				
	Gas flux (Tmol year^{-1})			
H_2	1 ± 0.5	$H_2 + 1/2O_2 \rightarrow H_2O$	0.5 ± 0.3	Catling and Kasting (2013), and references therein
CO	0.1 ± 0.05	$CO + 1/2O_2 \rightarrow CO_2$	0.05 ± 0.03	Catling and Kasting (2013), and references therein
H_2S	0.03 ± 0.015	$H_2S + 2O_2 \rightarrow H_2SO_4$	0.06 ± 0.03	Catling and Kasting (2013), and references therein
SO_2	1.8 ± 0.6	$H_2O + SO_2 + 1/2O_2 \rightarrow H_2SO_4$	0.9 ± 0.3	Catling and Kasting (2013), and references therein
Subtotal for surface volcanism = 1.5 ± 0.7				
Surface metamorphism				
CH_4 (abiotic)	0.3	$CH_4 + 2O_2 \rightarrow CO_2 + H_2O$	0.6	Fiebig et al. (2009)
CH_4 (thermogenic)	1.25	$CH_4 + 2O_2 \rightarrow CO_2 + H_2O$	2.5	Using the lower estimate of 1.25–2.5 Tmol CH_4 year^{-1} from Etiope et al. (2009)
Subtotal for metamorphic gases = 3.1				
Submarine volcanism				
H_2	0.1 ± 0.05	$H_2 + 1/2O_2 \rightarrow H_2O$	0.05 ± 0.03	
H_2S	0.35 ± 0.13	$H_2S + 2O_2 \rightarrow H_2SO_4$	0.7 ± 0.4	
CH_4 (ridge)	0.01 ± 0.005	$CH_4 + 2O_2 \rightarrow CO_2 + H_2O$	0.02 ± 0.01	
CH_4 (off axis)	0.25 ± 0.12	$CH_4 + 2O_2 \rightarrow CO_2 + H_2O$	0.5 ± 0.3	
Subtotal for submarine volcanic gases = 0.8 ± 0.7				
Seafloor oxidation and subduction				
Fe^{2+} conversion to magnetite		$12FeO + SO_4 \rightarrow 4Fe_3O_4 + S$	1.2 ± 0.3	Sleep (2005)
Total sink from subaerial and submarine reductants = 22.1 ± 8.4 Tmol year^{-1}				

$F_{metamorphic}$, which is the flux of O_2 consumed by reductants from metamorphism; and $F_{weathering}$, which is the flux of O_2 consumed by reduced minerals in seafloor and continental weathering. Today, R_{O_2} is 3.8×10^7 Tmol O_2 and the various source and sink fluxes in Tmol year^{-1} are shown in Tables 1 and 2. The average amount of time an O_2 molecule spends in the atmosphere–ocean system today is thus ~2 My, which is simply R_{O_2} divided by the source flux from Table 1 of ~18 Tmol O_2 year^{-1}. This timescale is clearly geologically short. In the past, any sustained difference between $F_{O_2 source}$ and $F_{O_2 sink}$ would have changed R_{O_2}.

6.7.2.5 The Definition of 'Anoxic' Versus 'Oxic' Atmospheres

Before considering the effect on the Earth's atmospheric chemistry of the GOE, the terms 'anoxic' and 'oxic' atmosphere are defined. Oxygen is absent from the atmospheres of many other celestial bodies, such as the giant planets and Saturn's largest moon, Titan. All of these atmospheres are 'anoxic.' But they also share another characteristic, which is that their redox chemistry is dominated by H_2 or hydrogen-bearing reducing gases, such as CH_4.

Hydrogen-bearing reducing gases (including hydrogen itself) behave as if they are the inverse of oxygen. Oxygen reacts rapidly with hydrogen-bearing reducing gases, so a decrease in the concentration of one allows an increase of the other. Anoxic atmospheres are all relatively rich in hydrogen-bearing reducing gases. There is 82.2 ± 2.6% H_2, 96.3 ± 2.4% H_2, ~82.5% H_2, and ~80% H_2 in the atmospheres of Jupiter, Saturn, Uranus, and Neptune, respectively, while Titan's lower atmosphere has ~5% CH_4. In contrast, Earth's current atmosphere (21% O_2, 1.8 ppmv CH_4) and that of Mars (0.13% O_2, 15 ppmv H_2) are both oxidizing. Given the observations of planetary atmospheres, it is clearly useful to define an 'anoxic' atmosphere as rich in hydrogen-bearing reducing gases and an oxic atmosphere as poor in hydrogen-bearing reducing gases.

The definition of anoxic versus oxic atmospheres helps people understand that the Archean atmosphere could have remained anoxic even if early oxygenic photosynthesis pumped O_2 into the atmosphere. Anoxia would have persisted if O_2 had been efficiently removed and overwhelmed by a flux of reducing gases into the atmosphere (including, in this tally, any flux of reducing cations in the ocean in communication with dissolved atmospheric O_2). Specifically, one can define an 'oxygenation parameter' as follows (Catling and Claire, 2005):

$$K_{oxy} = \frac{O_2 \text{ source flux}}{\text{non-weathering } O_2 \text{ sink flux}} = \frac{F_{reductant\_burial}}{F_{metamorphic} + F_{volcanic}} \; ; \begin{matrix} K_{oxy} > 1 \text{ gives an oxic atmosphere} \\ K_{oxy} < 1 \text{ gives an anoxic atmosphere} \end{matrix} \quad [12]$$

If this parameter exceeds unity, then O_2 in the atmosphere is quickly removed by reactions with reducing species. The result is that hydrogen-bearing reducing gases dominate the redox chemistry of the atmosphere even if there is a photosynthetic source of O_2. Detailed models that include photochemistry show that such a situation can occur (Claire et al., 2006; Pavlov et al., 2001; Zahnle et al., 2006).

6.7.3 Atmospheric Chemistry Through the Great Oxidation Event (GOE)

To understand the causes and consequences of the GOE, ideally, one would like to have time series concentrations of the redox-sensitive gases in the atmosphere (O_2, CH_4, and H_2) before and after the GOE. Information about the levels of other gases, such as CO_2, N_2O, and N_2, would also help in appreciating associated climate change. CO_2 and N_2O are greenhouse gases, while the concentration of N_2 modulates the size of the greenhouse effect through the pressure broadening of infrared absorption lines (Goldblatt et al., 2009). However, apart from some constraints on O_2 levels, there are very few reliable geologic determinations of the amounts of other gases. Most of the inferences are very indirect. Table 3 contains estimates of either concentrations or limits on concentrations of various atmospheric gases and marine sulfate. The basis for these estimates is described in the next two subsections.

6.7.3.1 Constraints on Atmospheric Gases Before the GOE

The strictest constraint on pre-GOE O_2 levels comes from mass-independent fractionation (MIF) of sulfur isotopes, which suggests that the O_2 level was less than about 1 ppmv in the Archean (Pavlov and Kasting, 2002; Zahnle et al., 2006). There are four stable isotopes of sulfur, ^{32}S, ^{33}S, ^{34}S, and ^{36}S. In mass-dependent fractionation (MDF), isotopes are fractionated according to the difference between their masses. Consequently, in MDF, ^{34}S is fractionated twice as much with respect to ^{32}S as is ^{33}S because the ^{34}S–^{32}S mass difference is twice that of ^{33}S–^{32}S. MDF applies to most fractionation processes, such as the diffusive separation of gases or the kinetics of microbial metabolism. Expressed in terms of the delta notation $\delta^x S = (^xS/^{32}S)_{sample}/(^xS/^{32}S)_{standard} - 1$, variations in $\delta^{33}S$ are usually about half those in $\delta^{34}S$ for MDF, which defines a

Table 3 A summary of approximate knowledge of species concentrations before and after the Great Oxidation Event (see text for sources)

Species	*Anoxic late Archean*	*Oxic middle Proterozoic*
Atmospheric O_2	<1 ppmv	0.2–2% by volume
Atmospheric CO_2	≤4%	≤0.4%
Atmospheric CH_4	~10^3 ppmv	~10^2 ppmv
Atmospheric N_2O	Unknown	Speculatively ~10–20 PAL
Atmospheric N_2	<1.9 PAL, speculatively lower than PAL	Unknown, speculatively similar to PAL
Marine SO_4^{2-}(aq)	<0.2 mM	~1–4 mM

PAL = present atmospheric level of a gas.

straight-line relationship. In contrast, MIF is any fractionation that deviates from the linear relationship. In simple terms,

$$\delta^{33}S \approx 0.5(\delta^{34}S) \text{ is mass-dependent fractionation (precisely, } \delta^{33}S = 0.515\delta^{34}S) \quad [13]$$

$$\delta^{33}S \neq 0.5(\delta^{34}S) \text{ is mass-independent fractionation (precisely, } \delta^{33}S \neq 0.515\delta^{34}S) \quad [14]$$

The proportionality constant can be considered ~0.5 for pedagogical purposes, but a more precise value is 0.515, as shown in parentheses earlier. Similarly, an MDF straight line defines the relationship of $\delta^{36}S$ and $\delta^{34}S$ as roughly $\delta^{36}S \approx 2\delta^{34}S$ or more precisely $\delta^{36}S = 1.90\delta^{34}S$.

A notation called 'cap delta' is used to express the magnitude of the MIF and refers to a deviation from the MDF straight line as follows:

$$\Delta^{33}S = \delta^{33}S - 0.515\delta^{34}S \quad [15]$$

$$\Delta^{36}S = \delta^{36}S - 1.9\delta^{34}S \quad [16]$$

A graph of $\Delta^{33}S$ for pyrites and sulfates over geologic time (see **Chapter 6.4**) shows an unambiguous step change around 2.4 Ga that has been interpreted as evidence for the rise of O_2 (Farquhar et al., 2000, 2010).

The relationship between MIF in sulfur isotopes and atmospheric redox chemistry arises because photochemistry is the only process capable of producing $\Delta^{33}S$ up to ~12‰, which is observed in the pre-GOE record. In the lab, large MIF is produced during photolysis of SO_2 and SO as follows (Farquhar et al., 2001):

$$SO_2 + h\nu = SO + O \quad [17]$$

$$SO + h\nu = S + O \quad [18]$$

The magnitude of the MIF depends on the isotopologue of the sulfur gas, that is, whether the gas is $^{32}SO_2$, $^{33}SO_2$, ^{32}SO, etc. (Danielache et al., 2008; Lyons, 2009). Little MIF is observed during the photolysis of H_2S. Given the strong absorption of short wavelength photons in the upper atmosphere by CO_2 and H_2O, for all practical purposes, the photons in the early atmosphere that induce photolysis in eqns [17] and [18] have wavelengths of 190–220 nm. Such ultraviolet photons can penetrate the troposphere in an anoxic atmosphere that lacks a stratospheric ozone layer. The elemental sulfur produced in eqn [18] polymerizes in anoxic atmospheres to make S_8 aerosols that rain out. However, sulfate aerosols are also produced from oxidizing pathways because CO_2 and H_2O are present in any realistic early Earth atmosphere and are a source of photochemical oxidants (eqn [1]). Consequently, sulfate and S_8 aerosols can rain out with MIF signatures of opposite sign in $\Delta^{33}S$ and can be segregated in the rock record because of different preservation pathways. Exactly how this process works is still a matter of research.

The presence of MIF in sulfur isotopes has various implications for the ancient atmospheric composition. In an oxic atmosphere, such as today's, the sulfur-containing gases are oxidized into sulfate, which is an isotopically homogenous single species with no MIF that rains out and washes to the ocean. Photochemical models show that the presence of MIF in sulfur isotopes requires three conditions as follows (Zahnle et al., 2006):

1. *Relatively abundant methane*. Photochemical models show that enough methane or hydrogen is needed as a reducing agent to form and precipitate S_8 from the upper troposphere (Ono et al., 2003). The presence of sulfur-MIF does not distinguish whether the reducing gas was hydrogen or methane. Certainly, H_2 is an expected biogenic gas as well as methane in the Archean (Hoehler et al., 2001). However, if the H_2 concentration had been more than $\sim 4 \times 10^{-5}$ bar, it would be consumed by biology at the Earth's surface and converted into methane, according to experiments (Kral et al., 1998). Also, biological thermodynamics predict atmospheric concentration ratios of CH_4/H_2 in the range 10–30 (Kasting et al., 2001). Consequently, it is reasonable to conclude that sulfur-MIF is indirect evidence that the Archean atmosphere was relatively rich in methane. Models suggest 10s–1000s ppmv, with the higher values giving larger rainout fluxes of S_8, presumably linked to larger $\Delta^{33}S$ values.
2. *Ground-level $O_2 < 1$ ppmv*. An anoxic atmosphere is required to allow the formation of both sulfate and S_8 aerosols that carry an S-MIF signal (Pavlov and Kasting, 2002). Also, lack of stratospheric ozone is required to allow sufficiently shortwave photons to photolyze tropospheric sulfur-bearing gases.
3. *Sufficient input of sulfur-bearing gases to the atmosphere*. The production rate of polymers of elemental sulfur scales with the amount of sulfur gases. The formation of S_2 polysulfur depends approximately on the square of the concentration of S produced from eqn [18] because it requires a reaction of the form S + S. By extrapolation, the production of S_8 aerosols should depend on the eighth power of sulfur concentrations, and so, S_8 production is clearly going to be very sensitive to fluxes of sulfur-bearing gases, as shown in photochemical models (Zahnle et al., 2006). Such gases include SO_2 from volcanism and possibly other S-bearing gases, perhaps biogenic ones.

The inference of trace levels of atmospheric O_2 is consistent with conventional geologic indicators of negligible O_2 in the Archean. These include the absence of continental red beds, the lack of oxidized paleosols, the presence of detrital minerals in riverbeds that would otherwise dissolve in oxygenated waters, and the ferruginous conditions in the deep ocean that gave rise to banded iron formations (BIFs) on continental shelves (see **Chapter 6.4**).

The record of $\Delta^{33}S$ over geologic time may also tell people about concentrations of other gases besides O_2 and CH_4. For example, if there had been very high CO_2, which is an efficient Rayleigh scatterer of UV, there would have been insufficient shortwave photons reaching the lower atmosphere to produce sulfur-MIF. Farquhar et al. (2001) suggest that levels of pCO_2 less than 0.8 bar were required for the presence of sulfur-MIF. This is consistent with a bound on the total atmospheric pressure of probably <1 bar deduced from fossil raindrop imprints at 2.7 Ga (Som et al., 2012).

In fact, there has been considerable debate about the amount of CO_2 versus methane in the Archean atmosphere. The general consensus is that Archean pCO_2 was higher than today but insufficient for CO_2–H_2O greenhouse warming of the early Earth without additional warming from other

greenhouse gases such as methane $\sim 10^3$ ppmv and its photochemical product, ethane (Haqq-Misra et al., 2008). Trace levels of ethane derived from methane turn out to be important because ethane absorbs in the atmospheric window region 8–12 μm where most of the Earth's infrared radiation otherwise escapes to space. Of course, photochemical models show that higher levels of methane and its photochemical products are expected in an anoxic atmosphere (Pavlov et al., 2000; Zahnle et al., 2006). The methane is assumed to be biogenic, which may have been enhanced by the leaching of nickel from abundant nickel-rich ultramafic rocks on the early Earth (Konhauser et al., 2009). Nickel is a key cofactor in several methanogen enzymes.

In an early study of paleosols (fossilized soils), Rye et al. (1995) suggested that $p\mathrm{CO_2}$ was no more than ~ 10 times the present levels based on the absence of siderite ($\mathrm{FeCO_3}$), which ought to form in anoxic pore waters in the presence of ferrous iron with higher $p\mathrm{CO_2}$. However, Sheldon (2006) criticized this paper. He found that calculated $p\mathrm{CO_2}$ would be comparable to modern levels (or even less) if up-to-date thermodynamic data were applied to the equilibrium between siderite and iron silicates proposed by Rye et al. Because of uncertainty about the exact silicate minerals in the equilibria, Sheldon suggested that the equilibria approach was flawed and that a mass balance approach was better. With mass balance, he derived an estimate of $23^{\times 3}_{\div 3}$ PAL of $\mathrm{CO_2}$ for 2.2 Ga paleosols, where his PAL (present atmospheric level) was taken as 370 ppmv $\mathrm{CO_2}$. Driese et al. (2011) applied the same method to a 2.69 Ga paleosol to derive a $p\mathrm{CO_2}$ of 10–50 PAL at that time.

The Driese et al. (2011) and Sheldon (2006) $p\mathrm{CO_2}$ estimates come from a paleosol weathering equation of Holland and Zbinden (1988):

$$\frac{M}{t}\ (\mathrm{mol\ cm^{-2}\ year^{-1}}) = \left[\frac{K_{\mathrm{CO_2}} \cdot r}{10^3} + \kappa \frac{D_{\mathrm{CO_2}} \cdot \alpha}{L}\right] p\mathrm{CO_2} \qquad [19]$$

On the right, the first term in the brackets accounts for $\mathrm{CO_2}$ dissolved in rainwater, while the second term corresponds to diffusion of $\mathrm{CO_2}$ through the soil. On the left is a column weathering rate where M is the number of moles of $\mathrm{CO_2}$ per $\mathrm{cm^2}$ required to produce the observed paleosol weathering profile and t is the soil formation time. The carbon dioxide partial pressure is $p\mathrm{CO_2}$ in atm; $K_{\mathrm{CO_2}}$ is the Henry's law constant for $\mathrm{CO_2}$; r is the amount of rainfall absorbed by the soil (cm $\mathrm{year^{-1}}$); κ is a conversion constant, that is, the ratio of seconds in a year divided by the number of $\mathrm{cm^3\ mol^{-1}}$ of gas at standard temperature and pressure ($=1.43\times10^3\ \mathrm{s\,cm^3\,(mol^{-1}\ year^{-1})}$); $K_{\mathrm{CO_2}}$ is the diffusion coefficient for $\mathrm{CO_2}$ in air ($0.162\ \mathrm{cm^2\,s^{-1}}$); α is the ratio of the $\mathrm{CO_2}$ diffusion coefficient in air to that in soil; and L is the total depth of the soil horizon. Holland and Zbinden assign an uncertainty of a factor of 10 in either direction on α, whereas Sheldon suggests that the biggest uncertainty is a factor of 2 in either direction in t, and he sets $\alpha = 0.1$ with a variability of $\pm 20\%$. Overall, the exact uncertainty on $p\mathrm{CO_2}$ obviously depends on assumptions about r, α, and t. But the general result is that $p\mathrm{CO_2}$ was probably up to 100 PAL but not higher in the late Archean. This constraint from paleosols is consistent with theoretical models that suggest greater hydrothermal alteration of the early seafloor basalt that may have removed $\mathrm{CO_2}$ and limited its abundance (Zahnle and Sleep, 2002).

In summary, the pre-GOE atmosphere likely had < 1 ppmv $\mathrm{O_2}$, high levels of methane $\sim 10^3$ ppmv (but possibly falling to ~ 10 ppmv around 2.4 Ga), and levels of $\mathrm{CO_2}$ up to 100 times the modern atmosphere's. Constraints on the amount of $\mathrm{N_2}$ remain very limited at present. Evidence from Archean fossil raindrop imprints suggests that the total pressure, $p\mathrm{N_2}$, was probably not much higher than today's level or perhaps lower (Som et al., 2012). A lower $p\mathrm{N_2}$ might be expected because the biogenic release of $\mathrm{N_2}$ to the atmosphere in the modern nitrogen cycle comes from nitrogen species that are oxidized prior to denitrification. This oxic part of the cycle would have been very limited when $\mathrm{O_2}$ was only a trace gas.

6.7.3.2 Constraints on Atmospheric Gases After the GOE

The Canadian geologist Stuart Roscoe first noticed that large glaciation events were associated with atmospheric redox change around 2.4 Ga (Roscoe, 1969). Roscoe's fieldwork was in the 2.45–2.22 Ga Huronian Supergroup of Canada, which is a section of mainly sedimentary rocks that contains detrital minerals of pyrite and uraninite stratigraphically below three diamictites. The diamictites are interpreted as evidence for three glaciations. Reduced detrital minerals, which should dissolve in oxygenated waters, suggest anoxic conditions before the glaciations. In addition, pre-2.45 Ga paleosols have upward depletion of total iron, which suggests weathering under an anoxic atmosphere that was able to mobilize $\mathrm{Fe^{2+}}$ in solution (Prasad and Roscoe, 1996). Pre-2.45 Ga Huronian paleosols also have cerium profiles indicative of anoxic weathering (Murakami et al., 2001). In contrast, the top of the Huronian succession contains red beds and oxidized paleosols. To Roscoe, such an association suggested a causal link between the atmospheric oxygenation and glaciations. Evidence for Paleoproterozoic glaciation is found in Australia, India, Russia, Scandinavia, South Africa, and elsewhere in North America (Bekker et al., 2003; Eyles and Young, 1994), which implies that it was global in extent. Moreover, the global climate is inferred to have been extremely cold because magnetic studies in the South African glaciations suggest low latitudes (Evans et al., 1997; Evans, 2003).

A possible explanation of the glaciations is that the rise of $\mathrm{O_2}$ could have diminished the greenhouse effect because an oxic atmosphere is chemically incompatible with comparatively large amounts of methane that should have existed in an anoxic atmosphere (Pavlov et al., 2000). A more nuanced view is that the gradual loss of reducing power in the late Archean atmosphere–ocean–crust system led to an increasing pool of seawater sulfate, smaller biogenic methane fluxes, and thus a decline of atmospheric methane levels that initiated the cooling of the Earth (Zahnle et al., 2006). Sulfur isotope evidence from the post-GOE glaciation supports this latter view (Papineau et al., 2007; Williford et al., 2011). Possibly, removal of $\mathrm{CO_2}$ through silicate weathering prior to the glacial times may have also contributed because of the subaerial occurrence of large igneous provinces at 2.45 Ga (Kump and Barley, 2007; Melezhik, 2006). In any case, the three Paleoproterozoic glacial episodes suggest that the atmosphere may have oscillated in composition and climate before finally settling down to a permanently oxic state. Some biogeochemical

models are able to reproduce such oscillations in atmospheric composition and climate (Claire et al., 2006). However, we note that the behavior of such models depends upon the parameterization of the response of biogenic O_2 and CH_4 fluxes to global temperature change. There remains great uncertainty about the magnitude and scaling of such a biogenic response to global climate.

In general, the persistent absence of significant S-MIF throughout the latter part of the Paleoproterozoic suggests that atmospheric O_2 concentrations must have increased to >1 ppmv. Although it is clear that the atmosphere was oxic, there are relatively few constraints on the exact O_2 levels. In the middle Proterozoic, the concentration of marine sulfate is inferred to have been at a level of a few mM compared to 28 mM today (Kah and Bartley, 2011; Kah et al., 2004; Shen et al., 2003), and it is likely that atmospheric O_2 levels stayed somewhere between $\sim$0.2% and 2% in absolute terms throughout much of the Proterozoic. It is only much later, by at least $\sim$551 Ma, that there are estimates of atmospheric O_2 >3% in absolute concentration. At that time, Canfield et al. (2007) calculate an O_2 level >3% by assuming an O_2 demand for 500–1500 m water depths of sediments at the Avalon Peninsula, Newfoundland. This Neoproterozoic rise in O_2 is also supported by a significant jump in Mo and V enrichments in black shales (Scott et al., 2008) along with δ^{98}Mo (Dahl et al., 2010).

A nonintuitive consequence of the rise of O_2 in the Paleoproterozoic was a probable reestablishment of atmospheric methane concentrations (Catling et al., 2004; Claire et al., 2006; Goldblatt et al., 2006) that were enough to produce $\sim$6–7 °C of greenhouse warming (Roberson et al., 2011). When O_2 rises and the stratospheric ozone layer is established, the net reaction between O_2 and methane in the troposphere slows down because the troposphere is shielded from shortwave UV (Catling et al., 2004; Claire et al., 2006; Goldblatt et al., 2006). Provided that there was a significant methane flux, the methane levels could have been as high as $\sim 10^2$ ppmv until the Neoproterozoic.

Today, there is an enormous flux of seafloor CH_4 that never reaches the atmosphere, estimated as a few tens of Tmol CH_4 year^{-1} (Catling et al., 2007). This methane is consumed by microbial SO_4^{2-} reduction at the CH_4–SO_4^{2-} transition zone in sediments (D'Hondt et al., 2002) so that the ocean is an inconsequential source of CH_4 for the modern atmosphere. But in a Proterozoic ocean with extensive euxinia, a big flux of methane could have vented from the seafloor to the atmosphere (Catling et al., 2002; Pavlov et al., 2003). Evidence for euxinia comes, in part, from molybdenum isotopes. Under high-oxygen conditions, uptake of Mo on marine solids preferentially removes ^{95}Mo relative to ^{98}Mo, leaving an isotopically heavy ocean. However, under low-oxygen conditions, seawater is ^{95}Mo-enriched. Sulfides in euxinic deep waters sequester Mo efficiently and can capture the marine Mo isotope composition. Rocks with ^{95}Mo enrichment from the 1.7–1.4 Ga McArthur Basin, Australia, suggest that the Mesoproterozoic deep ocean commonly had a euxinic area that was probably several percent compared to today's 0.3% (Arnold et al., 2004; Kendall et al., 2009, 2011).

Another redox-sensitive greenhouse gas that may have been moderately important after the GOE is nitrous oxide, N_2O (Buick, 2007). The source of N_2O is denitrification, when bacteria convert oxidized nitrogen compounds into N_2 along with minor N_2O release. The conversion of N_2O to N_2, which is the terminal step of denitrification, depends on the enzyme nitric oxide synthase, which contains 12 Cu atoms in its complex. Proterozoic oceans with widespread euxinia would tend to scavenge Cu into copper sulfides. If the oceans were copper-depleted, possibly more nitrogen was released as N_2O by a factor of 10–20. The concentration of N_2O roughly scales with its flux to the atmosphere. An N_2O level 10–20 times that of today's 0.3 ppmv could provide 3–5 °C of greenhouse warming (Roberson et al., 2011). Of course, there are no direct constraints on N_2O levels, but the Mesoproterozoic is an era with no evidence of glaciation, which suggests an unusual duration of climate stability and persistent greenhouse warming.

Carbon dioxide levels in the mid-Proterozoic were probably lower than those in the Archean and Paleoproterozoic. An analysis of paleosols from around 1.1–1.0 Ga suggests CO_2 levels $\leq$10 PAL (Mitchell and Sheldon, 2010; Sheldon, 2006). Also, microfossil evidence for *in vivo* calcification of cyanobacteria at 1.2 Ga suggests $pCO_2 \leq 10$ PAL (Kah and Riding, 2007). In contrast, paleosol analysis around 1.8 Ga implies CO_2 levels up to $\sim$50 PAL. **Table 3** summarizes the various estimates of gas concentrations before and after the GOE.

6.7.4 Explaining the Rise of O_2

A consideration of the meaning of anoxic versus oxic atmospheres (**Section 6.7.2.4**) allows deduction of what was required for a rise of O_2. If one examines eqn [11], it is clear that a positive value of $d[O_2]/dt$, that is, an O_2 increase, only occurs when the source of O_2 exceeds the O_2 sink. Alternatively, in terms of the parameter K_{oxy} introduced in eqn [12], to transition from an anoxic to oxic atmosphere, there are only two choices: either the O_2 source ($F_{reductant\_burial}$) increases or the nonweathering O_2 sink ($F_{metamorphic} + F_{volcanic}$) decreases. Consequently, various theories, described in the succeeding text, which attempt to explain the GOE, are all variants of these two themes.

6.7.4.1 Hypotheses for an Increasing Source of O_2

One group of hypotheses for the rise of O_2 concerns the idea that the source of O_2 increased because of enhanced rates of burial of organic carbon. These ideas divide into two subgroups: a pulse of organic burial caused the rise of O_2 or a long-term trend of increasing organic carbon burial led to a tipping point. Sometimes, the latter concept is tied to models of continental growth, where it is argued that more continental margin area allowed for more organic burial either directly or through nutrient supply.

At one end of the spectrum is the idea that the rise of O_2 happened almost immediately (in geologic time) after the origin of oxygenic photosynthesis (Kirschvink and Kopp, 2008). The counterargument is that there are multiple lines of independent evidence for the production of O_2 several hundred million years before the rise of O_2 at 2.4 Ga. Geochemical evidence of small amounts of O_2 before the GOE includes iron speciation in marine sediments (Kendall et al.,

2010; Poulton et al., 2010; Reinhard et al., 2009), trace amounts of molybdenum and rhenium (Anbar et al., 2007; Wille et al., 2007), sulfur isotope fractionation associated with the presence of sulfate (Kaufman et al., 2007), and extremely ^{12}C-enriched organic carbon consistent with microbes that oxidize methane with oxidants derived from O_2 or O_2 itself (Hayes, 1994; Hayes and Waldbauer, 2006). Although uncertain and controversial, organic biomarkers for cyanobacteria and steranes derived from steroids biosynthesized with O_2 are reported up to ~0.3 Gy before the rise of O_2 (Eigenbrode et al., 2008; Waldbauer et al., 2009). Conical stromatolites back to 2.7 Ga also indicate cyanobacterial production of O_2 through their disrupted, curled, and contorted laminae with enmeshed millimeter-scale bubbles (Bosak et al., 2009). Because one would need to dismiss all the earlier lines of evidence, the hypothesis of Kirschvink and Kopp (2008) has failed to garner much support in the Precambrian science community.

The idea that there was a pulse of burial of organic carbon arises from excursions in the carbon isotope record. Organic matter preferentially extracts the lighter isotope, ^{12}C, from the ocean so that seawater carbon, as recorded in marine carbonates, should become more ^{12}C-depleted (or higher in δ^{13}C) if organic burial rates increase. Two or three δ^{13}C excursions in carbonates occur during the period 2.4–2.06 Ga, including the global 2.2–2.06 Ga 'Lomagundi' excursion, named after a district in Zimbabwe (now called Makonde) where ^{13}C-rich dolomites were first studied (Bekker et al., 2006, 2008; Maheshwari et al., 2010; Melezhik and Fallick, 2010; Melezhik et al., 2007; Schidlowski et al., 1976). Karhu and Holland (1996) suggested that the Lomagundi carbonates indicated a pulse in organic carbon burial that may have caused the rise of O_2 because of associated O_2 release via eqn [9]. However, improved radiometric dating shows that the Lomagundi excursion cannot have caused the GOE because it happened 'after' the GOE at ~2.4 Ga. Instead, the excursion is probably an effect of the rise of O_2.

The remaining possibility (on the O_2 source side) is that there was a gradual increase of organic carbon burial. Whether or not this happened depends upon an interpretation of the somewhat noisy record of δ^{13}C in carbonates and organic carbon, for which there are differing views. One pioneering study suggested a secular increase in organic carbon burial fluxes based on boxcar averaging of the δ^{13}C time series (DesMarais et al., 1992). However, the averaging started at 2.6 Ga when very negative δ^{13}C for organic carbon ($\delta^{13}C_{org}$) occur. These anomalously low $\delta^{13}C_{org}$ values were subsequently attributed to methanotrophy (Hayes, 1994; Hayes and Waldbauer, 2006; Hinrichs and Boetius, 2002). If so, the $\delta^{13}C_{org}$ represents diagenetic processing in sediments rather than an isotopic balance involving global marine seawater. Another model concerns a gradual decrease of the uptake of ^{12}C-depleted carbon into hydrothermal carbonates from the early to late Archean, which would allow the fraction of organic carbon burial to increase within the constraints of the δ^{13}C record (Bjerrum and Canfield, 2004). This model assumes a gradient in the $^{13}C/^{12}C$ ratio between the surface and deep seawater from a 'biological pump.' However, of δ^{13}C, measurements in 3.46 Ga seafloor do not show such a gradient (Nakamura and Kato, 2004). Nonetheless, analysis of the carbon isotope data can produce a quite variable organic burial fraction over geologic time (see **Chapter 6.8**).

Continental shelves are places for burying organic carbon (Knoll, 1979), while continental weathering is a source of phosphorus, so some hypotheses of increasing organic burial tie organic burial to continental growth (Godderis and Veizer, 2000). Indeed, bursts of continental growth have been inferred from zircon U–Pb ages and speculatively linked to O_2 increases (Campbell and Allen, 2008). However, such bursts are probably artifacts of crustal preservation from supercontinent formation (Hawkesworth et al., 2009). Indeed, the present continental crust volume was probably reached by ~2–3 Ga (Hawkesworth et al., 2010), which, at least on the older end of these estimates, is 0.6 billion years before the GOE. For the younger end of this age range, the question is whether support is provided for a secular increase of organic burial by the δ^{13}C record or not.

6.7.4.2 Hypotheses for a Decreasing Sink of O_2

An alternative and fairly common interpretation of carbon isotopes is that there is no clear signal in the noisy record and that since 3.5 Ga, the average δ^{13}C value of marine carbonates has remained roughly constant at ~0‰, while the average $\delta^{13}C_{org}$ has been about −25‰ (Schidlowski, 1988). In this view, the fraction of carbon buried as organic relative to marine carbonate has remained roughly constant (Holland, 1984, 2002, 2009; Kump and Barley, 2007; Kump et al., 2001).

The fraction of carbon buried as organic carbon can be estimated from mass balance. On timescales exceeding ~10^5 years, which is the residence time of carbon on the ocean, the total amount of carbon entering the atmosphere–ocean system must balance the total amount leaving. Because the carbon is buried either as carbonate or organic carbon, the burial fractions of each type of carbon, f_{carb} and f_{org}, respectively, will sum to unity:

$$f_{carb} + f_{org} = 1 \qquad [20]$$

Similarly, the input and output flux must balance for the isotopic composition of carbon, however one expresses it, whether a $^{13}C/^{12}C$ ratio or δ^{13}C. So, in steady state, the isotopic composition of carbon input from mantle and riverine sources, $\delta^{13}C_{in}$, will equal the output, $\delta^{13}C_{out}$. One can expand eqn [20] to include the isotopic composition of organic matter, $\delta^{13}C_{org}$, and carbonates, $\delta^{13}C_{carb}$, as follows:

$$\begin{aligned}\delta^{13}C_{in} &= \delta^{13}C_{out} = f_{org}\delta^{13}C_{org} + f_{carb}\delta^{13}C_{carb} \\ &= f_{org}\delta^{13}C_{org} + (1 - f_{org})\delta^{13}C_{carb} = \delta^{13}C_{carb} - f_{org}\Delta_B\end{aligned} \qquad [21]$$

Here, Δ_B is the difference between carbonate and organic carbon isotopic composition:

$$\Delta_B = \delta^{13}C_{carb} - \delta^{13}C_{org} \qquad [22]$$

Consider the δ^{13}C values in the earlier equations. Today, volcanic gases show that mantle carbon has δ^{13}C around −5‰. This input value appears to have been constant over geologic time because ancient carbon in peridotitic xenoliths has δ^{13}C of about −5‰ (see **Chapter 3.5**), as does carbon in mantle-derived basalts and carbonatites (Mattey, 1987). Also, the riverine source from the weathering of organic carbon and carbonates

has a mean $\delta^{13}C$ value of about −5‰ as well (Holser et al., 1988). So, $\delta^{13}C_{in} \approx -5‰$. Marine sediments throughout geologic time have $\delta^{13}C_{carb} \approx 0‰$. While $\delta^{13}C_{org}$ has considerable scatter, it averages around −25‰ (Schidlowski, 1988). Thus, from eqn [22], one obtains $\Delta_B \approx 25‰$. Substituting this and other values into eqn [21], one has $-5‰ = 0 - f_{org}(25‰)$. Solving for f_{org}, one gets $f_{org} \sim 0.2$. Consequently, roughly 20% of incoming carbon is buried as organic carbon, while the remaining 80% fluxes out as carbonate carbon.

Given the relative constancy of average $^{13}C_{carb}$ and $\delta^{13}C_{org}$ since 3.5 Ga, some have argued for relative constancy of the ratio of the burial rates of organic and carbonate carbon (Holland, 1984, 2002, 2009; Kump and Barley, 2007; Kump et al., 2001). On the other hand, others have interpreted the data to suggest a larger magnitude of Δ_B in the Archean. For example, Hayes and Waldbauer (2006) suggest that f_{org} was ~0.15 throughout much of Earth's history and rose to ~0.24 since 0.9 Ga. Canfield (2005) also favors lower f_{org} in the Archean (see also **Chapter 6.8**).

If there had been relative constancy of the organic burial fraction within the error bars of the data and oxygen photosynthesis arose before 2.7 Ga, then the only way that Archean O_2 could remained a trace atmospheric gas is if there had been a large O_2 sink from a volcanic and metamorphic reductants (Catling et al., 2001; Holland, 2002; Kasting et al., 1993; Kump et al., 2001). Oxygen would have risen once the sink declined.

Following this line of logic, one group of hypotheses for the GOE suggests that there was a greater proportion of reducing gases in volcanic gases on the early Earth and that this fraction diminished in time. In other words, volcanic gases gradually became more oxidized (Holland, 2002; Kasting et al., 1993; Kump et al., 2001). Volcanic gases have a redox state that is controlled by the redox state of the mantle. Simply put, a more reducing mantle produces more reducing volcanic gases. So volcanic gases could have been more reducing in the Archean if the Archean mantle had been at a lower oxidation state than the Proterozoic mantle. However, analyses of redox-sensitive chromium and vanadium abundances in basalts (Canil, 2002; Delano, 2001; Li and Lee, 2004) indicate that the mantle's average oxidation state has remained roughly constant since ~3.5 Ga. This is somewhat surprising because it seems almost certain that the mantle has lost hydrogen to the atmosphere and then space (Catling et al., 2001; Kasting et al., 1993). However, the ability to lose reducing power and stay at the same oxidation state can be explained by the mantle's size and strong redox buffering (Lee et al., 2005).

The mantle redox state is expressed in terms of oxygen fugacity F_{O_2}. The term 'fugacity' generally represents the effective partial pressure of a gas in thermodynamic equilibrium with a particular mineral assemblage. But O_2 itself is not a gas species in rock. Instead, the dissociation of H_2O, CO_2, and SO_2 or the reduction of Fe^{3+} supplies oxidizing power, for which F_{O_2} is a theoretical index of the redox state (Frost, 1991). Petrologists define various synthetic mineral assemblages to characterize oxygen fugacities. These assemblages do not exist in nature but are used to express an equivalent F_{O_2} for natural assemblages. A common synthetic assemblage is the quartz–fayalite–magnetite (QFM or FMQ) buffer:

$$3Fe_2SiO_4 + O_2 \leftrightarrow 2Fe_3O_4 + 3SiO_2 \qquad [23]$$

The oxygen fugacity for this reaction is calculated as $F_{O_2} = 10^{-8.5}$, using a temperature- and pressure-dependent parameterization (Mueller and Saxena, 1977) with conditions appropriate for surface volcanism of 5 atm pressure and 1200 °C, or 1473.15 K (Holland, 1984).

Volcanic gases can be assumed to attain a redox state defined by the mantle oxygen fugacity. For example, the ratio of volcanic H_2 to steam will be determined by an equilibrium reaction as follows:

$$H_2O(g) \overset{K_{H_2O}}{\leftrightarrow} H_2 + \frac{1}{2}O_2 \qquad [24]$$

Here, K_{H_2O} is an equilibrium constant defined through the following:

$$K_{H_2O} = \frac{F_{H_2} \times F_{O_2}^{0.5}}{F_{H_2O}} \Rightarrow r_{H_2} = \frac{F_{H_2}}{F_{H_2O}} = \frac{K_{H_2O}}{F_{O_2}^{0.5}} \qquad [25]$$

In the second equality, r_{H_2} is ratio of the hydrogen and water fugacities, F_{H_2}/F_{H_2O}. Gibbs free energy values (available online from the US National Institute of Standards and Technology (NIST)) allow K_{H_2O} to be calculated as 1.31×10^{-6}. Consequently, substituting $F_{O_2} = 10^{-8.5}$ in eqn [25], one derives a modern value of r_{H_2} as ~0.02, which is similar to typical measured volcanic gas compositions (Holland, 1978). The geochemical studies mentioned earlier suggest that the average oxygen fugacity, F_{O_2}, in the Archean mantle differed from the modern mantle by no more than 0.3 $\log_{10}$ units. If F_{O_2} were 0.3 $\log_{10}$ units lower than $10^{-8.5}$, r_{H_2} would only increase to 0.03. Volcanic gases with ~3% of the hydrogen as H_2 compared to H_2O instead of ~2% today would make a negligible difference to the redox balance of the early atmosphere. Much larger changes in oxygen fugacity are necessary for significant effect. For example, if the Archean mantle F_{O_2} had been $10^{-11.5}$ atm, that is, 3 $\log_{10}$ units lower than today's $10^{-8.5}$, about three-quarters of volcanic hydrogen would have been emitted as H_2 rather than water vapor, providing a huge sink for O_2. But the geochemical data do not allow for such drastic F_{O_2} changes.

Although the mantle redox state has apparently remained roughly constant through time, it is still possible for the redox state of volcanic gases to have changed through other mechanisms. For example, consider the H_2/CO_2 flux ratio. The flux of H_2 is a sink on O_2, whereas the flux of CO_2 is related to the O_2 source flux because O_2 derives from carbon fixation and subsequent organic burial. In terms of fugacities, one can write

$$\frac{\text{Volcanic flux of } H_2}{\text{Volcanic flux of } CO_2} \approx \text{fugacity ratio} = \left(\frac{F_{H_2}}{F_{H_2O}}\right)\left[\frac{F_{H_2O}}{F_{CO_2}}\right] \approx r_{H_2}\left[\frac{H_2O \text{ flux}}{CO_2 \text{ flux}}\right] \qquad [26]$$

From eqn [26], one can see that if the flux ratio of H_2O/CO_2 through volcanoes changed in the past, the gas flux ratio of H_2/CO_2 would change even if r_{H_2} (the ratio of fugacities F_{H_2}/F_{H_2O}) had remained constant. Holland (2009) has put forward the hypothesis that carbon accumulated in the surface reservoir over time from outgassing so that the H_2O/CO_2 flux ratio through volcanoes decreased. In that case, the proportion of H_2 relative to the carbon outgassing would have been greater in the past, providing a larger sink on O_2. Holland also suggests

that the SO_2/H_2O flux ratio increased with time because of greater geologic cycling of sulfur. Certainly, after sulfate became abundant, subduction recycling of sulfur should have increased because people know that some seawater sulfur cycles through subduction zone volcanoes today. However, increased sulfur cycling is probably a positive feedback of the GOE, rather than its cause, because marine sulfate derives from the oxidation of sulfide. The history of carbon cycling is more complex. Some carbon cycle models establish a maximum surface reservoir of carbon by about 3 Ga (Zahnle and Sleep, 2002), which is much earlier than the GOE but there are many variables in such models.

Kump and Barley (2007) provide an alternative way to effect a change in the redox properties of volcanic gases. They suggest that the predominant style of volcanism evolved from submarine to subaerial. Submarine volcanism has a large area of relatively low-temperature, off-axis emissions that are more reducing than gases from high-temperature subaerial volcanism. Also, if there were shallower mid-ocean ridges, thermodynamics predicts a larger Fe^{2+} flux from hydrothermal vents compared to today, especially when seawater is depleted in sulfate (Kump and Seyfried, 2005). Today, the subaerial volcanic sink on O_2 is twice that of the submarine volcanic gas. Together, the subaerial and submarine volcanic sinks are a factor of $\sim$4 smaller than the O_2 flux released from organic burial according to inventories in **Table 2** versus **Table 1**. So the proposal of Kump and Barley (2007) requires large changes in the balance of volcanic emissions between subaerial and submarine. Another proposal on a similar theme is that the change in degassing pressure between submarine and subaerial volcanism shifted the redox state of the gases, based on model calculations (Gaillard et al., 2011). However, gas composition is sensitive to temperature, so the effect of reequilibration with lower-temperature surroundings as gases emerge from magmas requires further investigation.

A final and similar idea for a decreasing sink on O_2 is that the proportion of reducing gases in the metamorphic gas flux decreased from the Archean to the Proterozoic (Catling et al., 2001; Claire et al., 2006). Such gases, by definition, arise from regions in the crust that do not melt, and so, they are not constrained by the mantle redox.

A couple of chemical examples show how the crust could have lost hydrogen and become progressively oxidized. Some Archean BIFs (see **Chapter 6.6**) contain siderite ($FeCO_3$), which decomposes to magnetite during thermal metamorphism, as follows (McCollom, 2003):

$$12FeCO_3 + 2H_2O \rightarrow CH_4 + 11CO_2 + 4Fe_3O_4 \qquad [27]$$

In addition, serpentinization in hydrothermal systems generates hydrogen, which can be written schematically as

$$3FeO + H_2O \rightarrow Fe_3O_4 + H_2 \qquad [28]$$

Methane is often released from rocks where such serpentinization occurs because microbes convert the hydrogen into methane (Chapelle et al., 2002; Sherwood Lollar et al., 2006). Serpentinization certainly occurred in Archean greenstone belts, which are elongate regions with an abundance of altered mafic to ultramafic igneous rocks. In eqns [27] and [28], ferrous iron is oxidized to ferric iron and hydrogen-bearing gas is released. In the anoxic Archean atmosphere, high levels of methane or hydrogen would have necessarily caused a significant flux of hydrogen to escape to space (see **Section 6.7.2.1**). Subsequent metamorphic processing of the more oxidized crust would produce less reducing metamorphic gases as a matter of Le Chatelier's principle during each geologic cycle.

The proposal that the crust oxidized as a result of hydrogen loss is supported by inventories of oxidized and reduced species in the continental crust (**Figure 4**). If photosynthesis were solely responsible for the oxidation state of the crust, the number of moles of excess oxygen in ferric iron, sulfate, and free oxygen should be balanced by an equal number of moles of organic carbon (see eqn [9]). The continental crust, ocean, and atmosphere contain $\sim 2.5 \times 10^{21}$ mol of excess O_2 equivalents (Catling et al., 2001), which is mostly in the form of ferric iron that started out as ferrous iron. However, the quantity of reduced carbon in the crust is much smaller,

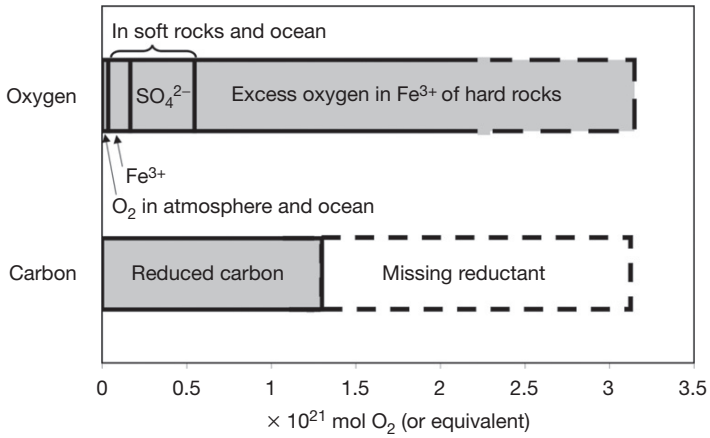

Figure 4 The inventory of oxygen in the Earth's crust. 'Hard rocks' are high-grade metamorphic rocks and igneous rocks. 'Soft rocks' are sedimentary rocks. The imbalance between oxygen and reduced carbon shows that there is a missing reductant (based on tabulated values in Catling et al., 2001 and references therein).

$<1.3 \times 10^{21}$ mol (Wedepohl, 1995). Hydrogen escape to space is a plausible explanation for the missing reductant because the expected quantity of oxidation is the correct size. If the concentration of methane in the Archean atmosphere had been $\sim 10^3$ ppmv, as calculated in photochemical models, the hydrogen escape rate would have been $\sim 7 \times 10^{12}$ mol O_2 year^{-1} from the theory of Section 6.7.2.1. Over 0.4 by, the escape of hydrogen at this rate would produce an irreversible quantity of 2.8×10^{21} mol O_2 equivalents – more than enough to account for the oxidation of the crust. Extra oxidation could have been taken up by the mantle with little effect on its overall redox state.

The overall result of a decline in the proportion of reducing gases in volcanic or metamorphic gases is the same: a transition to an oxic atmosphere. Claire et al. (2006) describe results of a box model that tracks the comings and goings of redox fluxes in the Earth system. The model includes parameterized photochemistry that allows calculation of the concentrations of atmospheric O_2 and methane. In this box model, crustal fugacity controls the oxidation state of metamorphic gases and, for numerical simplicity, the model converts organic carbon to Fe^{2+} equivalents via a process of greenschist metamorphism, $6Fe_2O_3 + C \rightarrow 4Fe_3O_4 + CO_2$. The model can be run assuming either that the volcanic gas sink diminished or that the metamorphic gas sink declined. Figure 5 shows that either scenario can generate an oxic transition. Common characteristics of such models are that there is negligible oxidative weathering prior to the GOE and that a transition to an oxic atmosphere occurs when K_{oxy} (as defined in eqn [12]) reaches unity.

6.7.5 Changes in Atmospheric Chemistry and Climate Associated with the Rise of O_2

6.7.5.1 The Collapse of Methane at the GOE

Earlier (Section 6.7.3.2), we discussed the possibility that a collapse of atmospheric methane levels was responsible for Paleoproterozoic glaciation. This would be consistent with increasing oxidation in the Earth system, particularly greater concentrations of sulfate in the ocean and diminished methane fluxes to the atmosphere as a result of methanotrophy using sulfate (Catling et al., 2007).

One can consider the biogeochemistry and associated atmospheric change in more detail. In the Archean microbial ecosystem models of Kasting et al. (2001) and Claire et al. (2006), the key redox-sensitive biogenic gases emitted to the atmosphere are O_2 and CH_4. Once oxygenic photosynthesis arose, it was the main source of sedimentary organic matter, which could be fermented by a consortium of microbes to make methane. The net reaction can be deduced as follows:

$$\begin{aligned} 2H_2O + 2CO_2 &\xrightarrow{\text{photosynthesis}} 2CH_2O + 2O_2 \\ 2CH_2O &\xrightarrow{\text{fermentation+methanogenesis}} CH_4 + CO_2 \\ \hline \text{Sum:} \quad {}^{-}CO_2 + 2H_2O &\rightarrow CH_4 + 2O_2 \end{aligned} \qquad [29]$$

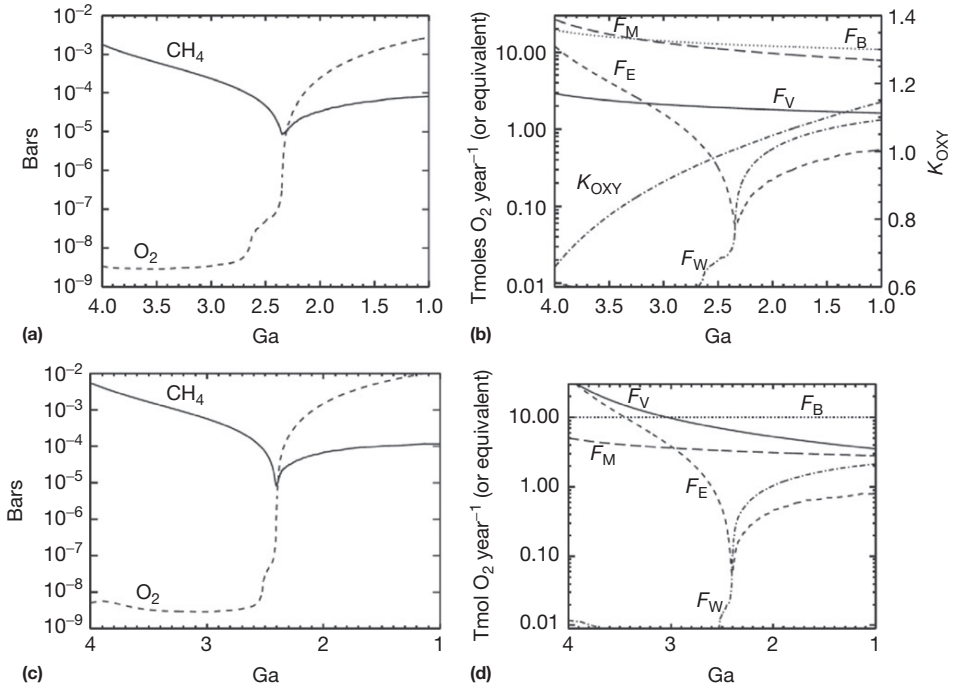

Figure 5 Results from the box model of Claire et al. (2006). (**a**, **b**) The upper row shows the results when the model assumes that metamorphic reducing gases are the primary sink on Archean O_2. (**c**, **d**) The lower row shows results where the model assumes that volcanic gases are the main O_2 sink. Qualitatively, there is no difference to the results from either assumption. Fluxes are as follows: F_W = continental oxidative weathering, F_E = hydrogen escape to space, F_V = volcanic sink, and F_M = metamorphic sink. K_{oxy} is the oxygenation parameter defined in the text, which reaches unity when the atmosphere goes through its 'Great Oxidation Event' (GOE).

Thus, oxygenic photosynthesis followed by fermentation and methanogenesis produces fluxes of $O_2(\phi_{O_2})$ and $CH_4(\phi_{CH_4})$ in the ratio $\phi_{O_2}/\phi_{CH_4} = 2$. Of course, methane is a relatively inert molecule, whereas O_2 reacts with a plethora of gases and soluble cations, particularly on a reducing early Earth. Consequently, one would not expect a simple 2:1 mutual destruction of O_2 and CH_4 but rather an atmosphere with negligible O_2 and relatively abundant methane, as data and models suggest. However, once standing pools of oxidants, such as marine sulfate, became more available, ϕ_{CH_4} should have dropped relative to ϕ_{O_2} because of methanotrophy (Valentine, 2002).

Photochemical models show that when the ϕ_{O_2}/ϕ_{CH_4} flux ratio increases, an atmosphere can flip to a permanently oxic state. Figure 6 shows the results of a photochemical model, which was run as a thought experiment. In this model, the ground-level methane abundance was held constant at 100 ppmv, while the ground-level O_2 mixing ratio was increased. The model calculated the fluxes of CH_4 and O_2 needed to maintain the prescribed atmosphere. This model used fixed outgassing fluxes of ~1 Tmol S $year^{-1}$ (with SO_2/H_2S in 10:1 ratio), 2.7 Tmol H_2 $year^{-1}$, and 0.3 Tmol CO $year^{-1}$. This outgassing sink on oxygen adds up to only ~2.15 Tmol O_2 $year^{-1}$, but one can think of it as a net flux that ignores the zero sum of an organic burial flux that would be of order ~10 Tmol O_2 $year^{-1}$ and a complementary ~10 Tmol O_2 $year^{-1}$ geologic gas sink. Figure 6 also shows the rainout fluxes of SO_4^{2-} and S_8 aerosols generated by the photochemistry. When the O_2 mixing ratio increases above 10^{-6}, that is, >1 ppm, one sees that the S_8 fallout flux drops off, which one interprets as related to the loss of MIF of sulfur isotopes (as described in Section 6.7.3.1). The plus symbols ('+') indicate the ϕ_{O_2}/ϕ_{CH_4} flux ratio, which maps to the right-hand vertical axis. In Figure 6, shaded regions require biogenic fluxes that Zahnle et al. (2006) argue are unreasonable. On the anoxic part of the graph, ϕ_{O_2}/ϕ_{CH_4} is ~2 but not precisely because there are fluxes of redox-sensitive rainout species, principally hydrogen peroxide and formaldehyde, which have to be tallied up to describe the atmosphere's redox budget precisely. Nonetheless, examination of Figure 6 shows that oxic solutions on the right have higher ϕ_{O_2}/ϕ_{CH_4} ratios than the anoxic solutions on the left. But the change is not much. An increase in the flux ratio ϕ_{O_2}/ϕ_{CH_4} of less than 3% creates a flip between an anoxic atmosphere with O_2 mixing ratio $\leq 2 \times 10^{-7}$ and an oxic atmosphere with O_2 mixing ratio $\geq 6 \times 10^{-4}$. Effectively, the increase in ϕ_{O_2}/ϕ_{CH_4} is equivalent to creating an imbalanced O_2 source where O_2 source exceeds the outgassing flux of reductants.

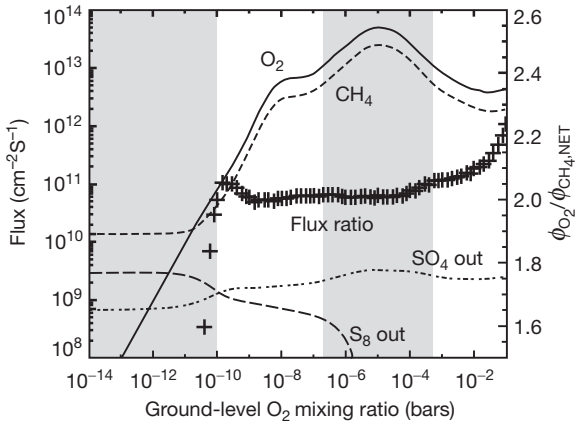

Figure 6 Atmospheric fluxes of chemical species as a function of the ground-level O_2 mixing ratio. Mixing ratio is equivalent to a partial pressure in bars for a 1 bar atmosphere. Results are shown from a photochemical 'thought experiment' where the ground-level CH_4 mixing ratio is fixed to 100 ppmv and volcanic outgassing fluxes of sulfur gases and reducing gases are also fixed (see text). Plus symbols ('+') map to the right-hand vertical axis and show the net ratio of the biogenic O_2 flux (ϕ_{O_2}) to CH_4 flux (ϕ_{CH_4}) as a function of the ground-level O_2 mixing ratio. The shaded regions represent cases when the biogenic O_2 fluxes are either implausibly high or low (from Catling et al., 2007).

6.7.5.2 The Formation of an Ozone Shield

After the GOE, the Earth was protected from shortwave ultraviolet by a stratospheric ozone layer. Stratospheric ozone (O_3) is derived from molecular oxygen. The photolysis of O_2 in the stratosphere produces oxygen atoms, which then combine with other O_2 molecules to make ozone, as follows:

$$O_2 + h\nu(\lambda < 242\ \text{nm}) \rightarrow O + O \quad [30]$$

$$O + O_2 + M \rightarrow O_3 + M \quad [31]$$

In eqn [31], 'M' is any air molecule – usually the most abundant one, N_2. 'M' removes energy liberated by the reaction, which is dissipated in molecular collisions. Ozone atoms formed in eqn [31] are able to absorb ultraviolet photons when they photolyze. Such absorption protects the Earth's surface from the biologically harmful range of ultraviolet wavelengths of 200–300 nm.

The ozone column abundance, that is, the number of molecules above a unit area of the Earth's surface, is related to how much UV can be absorbed. This column abundance has a nonlinear dependence on O_2 levels. Figure 7 shows the results of photochemical modeling (Kasting and Donahue, 1980). A relatively minor O_2 concentration ≥1% of the modern atmospheric level is sufficient to generate an ozone column that protects the surface from harmful ultraviolet. Thus, the small amount of O_2 expected after the GOE was enough to give rise to significant ozone shielding. This presumably would have expanded ecological niches for land-based life.

6.7.6 Conclusions

The concentration of an atmospheric gas is controlled by a kinetic competition between its production and loss. The GOE occurred because there was an imbalance between the O_2 source flux and the O_2 sink flux, which led to an accumulation of O_2 in the atmosphere. Several lines of evidence suggest that O_2 was being produced several hundred million years before the GOE at 2.4 Ga (see Chapter 6.4). However, the Archean atmosphere would have remained anoxic if O_2 consumption fluxes exceeded the long-term source of O_2 from the flux of organic carbon burial. In an anoxic atmosphere, the loss of O_2 to continental oxidative weathering is negligible, so the dominant sinks on O_2 in the Archean must have been reactions with volcanic and metamorphic reductants, including reducing gases (H_2, CH_4, CO, SO_2, and H_2S) and dissolved reducing cations (e.g., Fe^{2+}) in direct communication with the atmosphere. A 'tipping point'

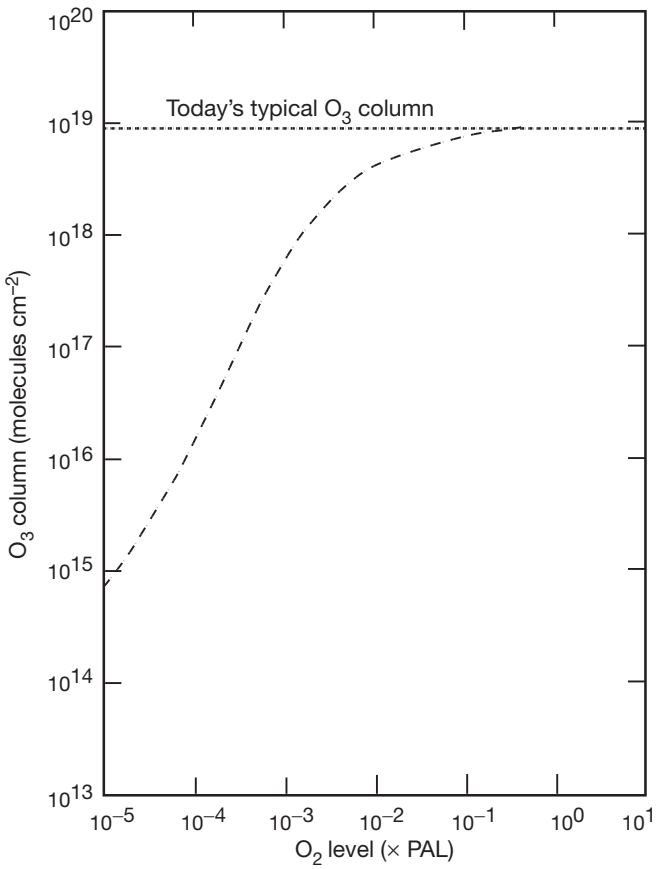

Figure 7 The ozone (O_3) column abundance shown as the dashed line as a function of the concentration of ground-level atmospheric oxygen. The O_2 level is expressed as a ratio to the present atmospheric level (PAL). Today's typical ozone column abundance is shown as a dotted line. The ozone layer's protective absorption of biologically harmful ultraviolet radiation becomes significant at $\sim 10^{-2}$ PAL.

would have been reached when the flux of O_2 from organic carbon burial exceeded the O_2 loss to volcanic and metamorphic sinks. After the GOE, oxidative weathering was a significant new sink on O_2 and helped set its new level.

In the redox chemistry of the atmosphere, hydrogen-bearing reduced gases (such as CH_4 and H_2) are the chemical adversaries of O_2. When the concentration of one goes up, the other declines, and vice versa. Photochemical reactions cause rapid mutual annihilation between O_2 and the reducing gases. In general, people expect the redox chemistry of the pre-GOE atmosphere to have been dominated by methane and hydrogen (even though they were both probably at levels below a percent), whereas O_2 would have been a trace gas at less than 1 ppmv. It is opposite to the redox control in the modern atmosphere. Models suggest that the GOE occurred when the rate of supply of reduced gases to the atmosphere dropped below the O_2 flux to the atmosphere (Claire et al., 2006; Goldblatt et al., 2006; Holland, 2009).

The GOE appears in the rock record at the same time as global cooling. In detailed models of the GOE, there is a decline in the supply of reducing gases prior to the GOE, which means that the methane concentration in the pre-GOE atmosphere falls to low levels even before O_2 rises to a substantial concentration (Zahnle et al., 2006). The loss of greenhouse gases such as methane and its photochemical product, ethane, is plausibly responsible for global cooling at ~2.4 Ga. It is possible that the global climate and atmospheric composition oscillated until conditions of permanent oxygenation were established, which would account for multiple glaciations during 2.45–2.22 Ga.

Moderate levels of O_2 established in the Proterozoic (probably somewhere between 0.2% and 2% O_2 by volume) were sufficient to establish a stratospheric ozone (O_3) layer (Kasting and Donahue, 1980) and protect the Earth's surface from harmful ultraviolet in the range 200–300 nm. A counterintuitive effect of the ozone layer was to decrease the net reaction rate in the troposphere between methane and oxygen. Provided that methane fluxes were still relatively large from a poorly oxygenated and euxinic Proterozoic ocean, methane should have risen after the GOE to be a moderately significant greenhouse gas during middle Proterozoic.

Acknowledgments

The author thanks Shawn Domagal-Goldman for improving the manuscript and NASA Astrobiology/Exobiology Program grant NNX10AQ90G for the support.

References

Anbar AD, Duan Y, Lyons TW, et al. (2007) A whiff of oxygen before the Great Oxidation Event? *Science* 317: 1903–1906.

Arnold GL, Anbar AD, Barling J, and Lyons TW (2004) Molybdenum isotope evidence for widespread anoxia in mid-Proterozoic oceans. *Science* 304: 87–90.

Bekker A, Holmden C, Beukes NJ, Kenig F, Eglingtone B, and Patterson WP (2008) Fractionation between inorganic and organic carbon during the Lomagundi (2.22-2.1 Ga) carbon isotope excursion. *Earth and Planetary Science Letters* 271: 278–291.

Bekker A, Karhu JA, Eriksson KA, and Kaufman AJ (2003) Chemostratigraphy of Paleoproterozoic carbonate successions of the Wyoming Craton: Tectonic forcing of biogeochemical change? *Precambrian Research* 120: 279–325.

Bekker A, Karhu JA, and Kaufman AJ (2006) Carbon isotope record for the onset of the Lomagundi carbon isotope excursion in the Great Lakes area, North America. *Precambrian Research* 148: 145–180.

Berner RA (1982) Burial of organic-carbon and pyrite sulfur in the modern ocean - Its geochemical and environmental significance. *American Journal of Science* 282: 451–473.

Berner RA (2004) *The Phanerozoic Carbon Cycle*. New York: Oxford University Press.

Bjerrum CJ and Canfield DE (2004) New insights into the burial history of organic carbon on the early Earth. *Geochemistry Geophysics Geosystems* 5: 2004Gc000713.

Bosak T, Liang B, Sim MS, and Petroff AP (2009) Morphological record of oxygenic photosynthesis in conical stromatolites. *Proceedings of the National Academy of Sciences of the United States of America* 106: 10939–10943.

Buick R (2007) Did the Proterozoic 'Canfield Ocean' cause a laughing gas greenhouse? *Geobiology* 5: 97–100.

Campbell IH and Allen CM (2008) Formation of supercontinents linked to increases in atmospheric oxygen. *Nature Geoscience* 1: 554–558.

Canfield DE (2005) The early history of atmospheric oxygen: Homage to Robert A. Garrels. *Annual Review of Earth and Planetary Sciences* 33: 1–36.

Canfield DE, Poulton SW, and Narbonne GM (2007) Late-Neoproterozoic deep-ocean oxygenation and the rise of animal life. *Science* 315: 92–95.

Canil D (2002) Vanadium in peridotites, mantle redox and tectonic environments: Archean to present. *Earth and Planetary Science Letters* 195: 75–90.

Catling DC and Claire MW (2005) How Earth's atmosphere evolved to an oxic state: A status report. *Earth and Planetary Science Letters* 237: 1–20.

Catling DC, Claire MW, and Zahnle KJ (2004) Understanding the evolution of atmospheric redox state from the Archaean to the Proterozoic. In: Reimold WU and Hofmann A (eds.) *Field Forum on Processes on the Early Earth*, pp. 17–19. Kaapvaal Craton: University of Witwatersrand.

Catling DC, Claire MW, and Zahnle KJ (2007) Anaerobic methanotrophy and the rise of atmospheric oxygen. *Philosophical Transactions of the Royal Society of London. Series B, Biological Sciences* A365: 1867–1888.

Catling DC and Kasting JF (~~2013~~) *Atmospheric Evolution on Inhabited and Lifeless Worlds*. New York, Cambridge University Press (expected 2014).

Catling DC, Zahnle KJ, and McKay CP (2001) Biogenic methane, hydrogen escape, and the irreversible oxidation of early Earth. *Science* 293: 839–843.

Catling DC, Zahnle KJ, and McKay CP (2002) What caused the second rise of O_2 in the late Proterozoic? Methane, sulfate, and irreversible oxidation. *Astrobiology* 2: 569 (Abstract).

Chapelle FH, O'Neill K, Bradley PM, et al. (2002) A hydrogen-based subsurface microbial community dominated by methanogens. *Nature* 415: 312–315.

Claire MW (2008) *Quantitative Modeling of the Rise in Atmospheric Oxygen*. PhD Thesis. Seattle: University of Washington.

Claire MW, Catling DC, and Zahnle KJ (2006) Biogeochemical modeling of the rise of oxygen. *Geobiology* 4: 239–269.

D'Hondt S, Rutherford S, and Spivack AJ (2002) Metabolic activity of subsurface life in deep-sea sediments. *Science* 295: 2067–2070.

Dahl TW, Hammarlund EU, Anbar AD, et al. (2010) Devonian rise in atmospheric oxygen correlated to the radiations of terrestrial plants and large predatory fish. *Proceedings of the National Academy of Sciences of the United States of America* 107: 17911–17915.

Danielache SO, Eskebjerg C, Johnson MS, Ueno Y, and Yoshida N (2008) High-precision spectroscopy of ^{32}S, ^{33}S, and ^{34}S sulfur dioxide: Ultraviolet absorption cross sections and isotope effects. *Journal of Geophysical Research* 113: D17314.

Delano JW (2001) Redox history of the Earth's interior: Implications for the origin of life. *Origins of Life and Evolution of the Biosphere* 31: 311–341.

DesMarais DJ, Strauss H, Summons RE, and Hayes JM (1992) Carbon isotope evidence for the stepwise oxidation of the Proterozoic environment. *Nature* 359: 605–609.

Driese SG, Jirsa MA, Ren MH, et al. (2011) Neoarchean paleoweathering of tonalite and metabasalt: Implications for reconstructions of 2.69 Ga early terrestrial ecosystems and paleoatmospheric chemistry. *Precambrian Research* 189: 1–17.

Eigenbrode JL, Freeman KH, and Summons RE (2008) Methylhopane biomarker hydrocarbons in Hamersley Province sediments provide evidence for Neoarchean aerobiosis. *Earth and Planetary Science Letters* 273: 323–331.

Etiope G, Feyzullayev A, and Baciu CL (2009) Terrestrial methane seeps and mud volcanoes: A global perspective of gas origin. *Marine and Petroleum Geology* 26: 333–344.

Evans DA, Beukes NJ, and Kirshvink JL (1997) Low-latitude glaciation in the Proterozoic era. *Nature* 386: 262–266.

Evans DAD (2003) A fundamental Precambrian-Phanerozoic shift in earth's glacial style? *Tectonophysics* 375: 353–385.

Eyles N and Young GM (1994) Geodynamic controls on glaciation in Earth's history. In: Deynous M, Miler JMG, Domack EW, Eyles N, Fairchild IJ, and Young GM (eds.) *Earth's Glacial Record*, pp. 1–28. New York: Cambridge University Press.

Farquhar J, Bao H, and Thiemans M (2000) Atmospheric influence of Earth's earliest sulfur cycle. *Science* 289: 756–758.

Farquhar J, Savarino J, Airieau S, and Thiemens MH (2001) Observation of wavelength-sensitive mass-independent sulfur isotope effects during SO_2 photolysis: Application to the early atmosphere. *Journal of Geophysical Research* 106: 1–11.

Farquhar J, Wu NP, Canfield DE, and Oduro H (2010) Connections between sulfur cycle evolution, sulfur isotopes, sediments, and base metal sulfide deposits. *Economic Geology* 105: 509–533.

Fiebig J, Woodland AB, D'Alessandro W, and Puttmann W (2009) Excess methane in continental hydrothermal emissions is abiogenic. *Geology* 37: 495–498.

Frost BR (1991) Introduction to oxygen fugacity and its petrologic importance. In: Lindsley DH (ed.) *Reviews in Mineralogy* 25: pp. 1–9. Washington, DC: Mineralogical Society of America.

Gaillard F, Scaillet B, and Arndt NT (2011) Atmospheric oxygenation caused by a change in volcanic degassing pressure. *Nature* 478: 229-U112.

Godderis Y and Veizer J (2000) Tectonic control of chemical and isotopic composition of ancient oceans: The impact of continental growth. *American Journal of Science* 300: 434–461.

Goldblatt C, Claire MW, Lenton TM, Matthews AJ, Watson AJ, and Zahnle KJ (2009) Nitrogen-enhanced greenhouse warming on early Earth. *Nature Geoscience* 2: 891–896.

Goldblatt C, Lenton TM, and Watson AJ (2006) Bistability of atmospheric oxygen and the Great Oxidation. *Nature* 443: 683–686.

Hall DT, Feldman PD, McGrath MA, and Strobel DF (1998) The far-ultraviolet oxygen airglow of Europa and Ganymede. *The Astrophysical Journal* 499: 475–481.

Haqq-Misra JD, Domagal-Goldman SD, Kasting PJ, and Kasting JF (2008) A revised, hazy methane greenhouse for the Archean Earth. *Astrobiology* 8: 1127–1137.

Harries J, Ruth S, and Russell JM (1996) On the distribution of mesospheric molecular hydrogen inferred from HALOE measurements of H_2O and CH_4. *Geophysical Research Letters* 23: 297–300.

Hawkesworth C, Cawood P, Kemp T, Storey C, and Dhuime B (2009) A matter of preservation. *Science* 323: 49–50.

Hawkesworth CJ, Dhuime B, Pietranik AB, Cawood PA, Kemp AIS, and Storey CD (2010) The generation and evolution of the continental crust. *Journal of the Geological Society* 167: 229–248.

Hayes JM (1994) Global methanotrophy at the Archean-Preoterozoic transition. In: Bengtson S (ed.) *Early Life on Earth*, pp. 220–236. New York: Columbia University Press.

Hayes JM and Waldbauer JR (2006) The carbon cycle and associated redox processes through time. *Philosophical Transactions of the Royal Society of London. Series B, Biological Sciences* 361: 931–950.

Hinrichs KU and Boetius A (2002) The anaerobic oxidation of methane: New insights in microbial ecology and biogeochemistry. In: Wefer G, Billett D, Hebbeln D, Jorgensen BB, Schluter M, and Van Weering T (eds.) *Ocean Margin Systems*, pp. 457–477. Berlin: Springer.

Hoehler TM, Bebout BM, and DesMarais DJ (2001) The role of microbial mats in the production of reduced gases on the early Earth. *Nature* 412: 324–327.

Holland HD (1978) *The Chemistry of the Atmosphere and Oceans*. New York: Wiley.

Holland HD (1984) *The Chemical Evolution of the Atmosphere and Oceans*. Princeton, NJ: Princeton University Press.

Holland HD (2002) Volcanic gases, black smokers, and the Great Oxidation Event. *Geochimica et Cosmochimica Acta* 66: 3811–3826.

Holland HD (2009) Why the atmosphere became oxygenated: A proposal. *Geochimica et Cosmochimica Acta* 73: 5241–5255.

Holland HD and Zbinden EA (1988) Paleosols and the evolution of the atmosphere: Part I. In: Lerman A and Meybeck M (eds.) *Physical and Chemical Weathering in Geochemical Cycles*, pp. 61–82. Dordrecht: Reidel.

Holser WT, Schidlowski M, Mackenzie FT, and Maynard JB (1988) Geochemical cycles of carbon and sulfur. In: Gregor CB, Garrels RM, Mackenzie FT, and Maynard JB (eds.) *Chemical Cycles in the Evolution of the Earth*, pp. 105–173. New York: Wiley.

Hunten DM (1973) The escape of light gases from planetary atmospheres. *Journal of the Atmospheric Sciences* 30: 1481–1494.

Hunten DM (1979) Possible oxidant sources in the atmosphere and surface of Mars. *Journal of Molecular Evolution* 14: 71–78.

Hunten DM (1990) Kuiper Prize Lecture: Escape of atmospheres, ancient and modern. *Icarus* 85: 1–20.

Kah LC and Bartley JK (2011) Protracted oxygenation of the Proterozoic biosphere. *International Geology Review* 53: 1424–1442.

Kah LC, Lyons TW, and Frank TD (2004) Low marine sulphate and protracted oxygenation of the Proterozoic biosphere. *Nature* 431: 834–838.

Kah LC and Riding R (2007) Mesoproterozoic carbon dioxide levels inferred from calcified cyanobacteria. *Geology* 35: 799–802.

Karhu JA and Holland HD (1996) Carbon isotopes and the rise of atmospheric oxygen. *Geology* 24: 867–870.

Kasting JF and Donahue TM (1980) The evolution of atmospheric ozone. *Journal of Geophysical Research* 85: 3255–3263.

Kasting JF, Eggler DH, and Raeburn SP (1993) Mantle redox evolution and the oxidation state of the Archean atmosphere. *Journal of Geology* 101: 245–257.

Kasting JF, Pavlov AA, and Siefert JL (2001) A coupled ecosystem-climate model for predicting the methane concentration in the Archean atmosphere. *Origins of Life and Evolution of the Biosphere* 31: 271–285.

Kaufman AJ, Johnston DT, Farquhar J, et al. (2007) Late Archean biospheric oxygenation and atmospheric evolution. *Science* 317: 1900–1903.

Kendall B, Creaser RA, Gordon GW, and Anbar AD (2009) Re-Os and Mo isotope systematics of black shales from the Middle Proterozoic Velkerri and Wollogorang Formations, McArthur Basin, northern Australia. *Geochimica et Cosmochimica Acta* 73: 2534–2558.

Kendall B, Gordon GW, Poulton SW, and Anbar AD (2011) Molybdenum isotope constraints on the extent of late Paleoproterozoic ocean euxinia. *Earth and Planetary Science Letters* 307: 450–460.

Kendall B, Reinhard CT, Lyons T, Kaufman AJ, Poulton S, and Anbar AD (2010) Pervasive oxygenation along late Archaean ocean margins. *Nature Geoscience* 3: 647–652.

Kirschvink JL and Kopp RE (2008) Palaeoproterozoic ice houses and the evolution of oxygen-mediating enzymes: The case for a late origin of photosystem II. *Philosophical Transactions of the Royal Society of London. Series B, Biological Sciences* 363: 2755–2765.

Knoll AH (1979) Archean photoautotrophy - Some alternatives and limits. *Origins of Life and Evolution of the Biosphere* 9: 313–327.

Konhauser KO, Pecoits E, Lalonde SV, et al. (2009) Oceanic nickel depletion and a methanogen famine before the Great Oxidation Event. *Nature* 458: 750-U85.

Kral TA, Brink KM, Miller SL, and McKay CP (1998) Hydrogen consumption by methanogens on the early Earth. *Origins of Life and Evolution of the Biosphere* 28: 311–319.

Kump LR and Barley ME (2007) Increased subaerial volcanism and the rise of atmospheric oxygen 2.5 billion years ago. *Nature* 448: 1033–1036.

Kump LR, Kasting JF, and Barley ME (2001) The rise of atmospheric oxygen and the "upside-down" Archean mantle. *Geochemistry, Geophysics, Geosystems* 2 (on line).

Kump LR and Seyfried WE (2005) Hydrothermal Fe fluxes during the Precambrian: Effect of low oceanic sulfate concentrations and low hydrostatic pressure on the composition of black smokers. *Earth and Planetary Science Letters* 235: 654–662.

Lee CTA, Leeman WP, Canil D, and Li ZXA (2005) Similar V/Sc systematics in MORB and arc basalts: Implications for the oxygen fugacities of their mantle source regions. *Journal of Petrology* 46: 2313–2336.

Li ZXA and Lee CTA (2004) The constancy of upper mantle fO(2) through time inferred from V/Sc ratios in basalts. *Earth and Planetary Science Letters* 228: 483–493.

Lyons JR (2009) Atmospherically-derived mass-independent sulfur isotope signatures, and incorporation into sediments. *Chemical Geology* 267: 164–174.

Maheshwari A, Sial AN, Gaucher C, et al. (2010) Global nature of the Paleoproterozoic Lomagundi carbon isotope excursion: A review of occurrences in Brazil, India, and Uruguay. *Precambrian Research* 182: 274–299.

Mattey DP (1987) Carbon isotopes in the mantle. *Terra Cognita* 7: 31–37.

McCollom TM (2003) Formation of meteorite hydrocarbons from thermal decomposition of siderite ($FeCO_3$). *Geochimica et Cosmochimica Acta* 67: 311–317.

Melezhik VA (2006) Multiple causes of Earth's earliest global glaciation. *Terra Nova* 18: 130–137.

Melezhik VA and Fallick AE (2010) On the Lomagundi-Jatuli carbon isotopic event: The evidence from the Kalix Greenstone Belt, Sweden. *Precambrian Research* 179: 165–190.

Melezhik VA, Huhma H, Condon DJ, Fallick AE, and Whitehouse MJ (2007) Temporal constraints on the Paleoproterozoic Lomagundi-Jatuli carbon isotopic event. *Geology* 35: 655–658.

Mitchell RL and Sheldon ND (2010) The 1100 Ma Sturgeon Falls paleosol revisited: Implications for Mesoproterozoic weathering environments and atmospheric CO_2 levels. *Precambrian Research* 183: 738–748.

Mueller RF and Saxena SK (1977) *Chemical Petrology*. New York: Springer.

Murakami T, Utsunomiya S, Imazu Y, and Prasad N (2001) Direct evidence of Late Archean to Early Proterozoic anoxic atmosphere from a product of 2.5 Ga old weathering. *Earth and Planetary Science Letters* 184: 523.

Nakamura K and Kato Y (2004) Carbonatization of oceanic crust by the seafloor hydrothermal activity and its significance as a CO_2 sink in the Early Archean. *Geochimica et Cosmochimica Acta* 68: 4595–4618.

Ono S, Eigenbrode JL, Pavlov AA, et al. (2003) New insights into Archean sulfur cycle from mass-independent sulfur isotope records from the Hamersley Basin, Australia. *Earth and Planetary Science Letters* 213: 15–30.

Papineau D, Mojzsis SJ, and Schmitt AK (2007) Multiple sulfur isotopes from Paleoproterozoic Huronian interglacial sediments and the rise of atmospheric oxygen. *Earth and Planetary Science Letters* 255: 188–212.

Pavlov AA, Hurtgen MT, Kasting JF, and Arthur MA (2003) Methane-rich Proterozoic atmosphere? *Geology* 31: 87–90.

Pavlov AA and Kasting JF (2002) Mass-independent fractionation of sulfur isotopes in Archean sediments: Strong evidence for an anoxic Archean atmosphere. *Astrobiology* 2: 27–41.

Pavlov AA, Kasting JF, and Brown LL (2001) UV-shielding of NH_3 and O_2 by organic hazes in the Archean atmosphere. *Journal of Geophysical Research* 106: 23267–23287.

Pavlov AA, Kasting JF, Brown LL, Rages KA, and Freedman R (2000) Greenhouse warming by CH_4 in the atmosphere of early Earth. *Journal of Geophysical Research* 105: 11981–11990.

Poulton SW, Fralick PW, and Canfield DE (2010) Spatial variability in oceanic redox structure 1.8 billion years ago. *Nature Geoscience* 3: 486–490.

Prasad N and Roscoe SM (1996) Evidence of anoxic to oxic atmosphere change during 2.45-2.22 Ga from lower and upper sub-Huronian paleosols Canada. *Catena* 27: 105–121.

Reinhard CT, Raiswell R, Scott C, Anbar AD, and Lyons TW (2009) A late archean sulfidic sea stimulated by early oxidative weathering of the continents. *Science* 326: 713–716.

Roberson AL, Roadt J, Halevy I, and Kasting JF (2011) Greenhouse warming by nitrous oxide and methane in the Proterozoic Eon. *Geobiology* 9: 313–320.

Roscoe SM (1969) Huronian rocks and uraniferous conglomerates in the Canadian Shield. Geological Survey of Canada Paper 68-40, p. 205.

Rye R, Kuo PH, and Holland HD (1995) Atmospheric carbon dioxide concentrations before 2.2 billion years ago. *Nature* 378: 603–605.

Schidlowski M (1988) A 3,800-million-year isotopic record of life from carbon in sedimentary rocks. *Nature* 333: 313–318.

Schidlowski M, Eichmann R, and Junge CE (1976) Carbon isotope geochemistry of Precambrian Lomagundi carbonate province Rhodesia. *Geochimica et Cosmochimica Acta* 40: 449–455.

Scott C, Lyons TW, Bekker A, et al. (2008) Tracing the stepwise oxygenation of the Proterozoic ocean. *Nature* 452: 456-U5.

Sheldon ND (2006) Precambrian paleosols and atmospheric CO_2 levels. *Precambrian Research* 147: 148–155.

Shen Y, Knoll AH, and Walter MR (2003) Evidence for low sulphate and anoxia in a mid-Proterozoic marine basin. *Nature* 423: 632–635.

Sherwood Lollar B, Lacrampe-Couloume G, Slater GF, et al. (2006) Unravelling abiogenic and biogenic sources of methane in the Earth's deep subsurface. *Chemical Geology* 226: 328–339.

Sleep NH (2005) Dioxygen over geologic time. In: Sigel A, Sigel H, and Sigel R (eds.) *Metal Ions in Biological Systems, Vol. 43: Biogeochemical Cycles of Elements*, pp. 49–73. Boca Raton, FL: Taylor & Francis.

Smyth WH and Marconi ML (2006) Europa's atmosphere, gas tori, and magnetospheric implications. *Icarus* 181: 510–526.

Som SM, Catling DC, Harnmeijer JP, et al. (2012) Air density 2.7 Gyr ago limited to less than twice modern levels by fossil raindrop imprints. *Nature* 484: 359–362.

Teolis BD, Jones GH, Miles PF, et al. (2010) Cassini Finds an oxygen-carbon dioxide atmosphere at Saturn's icy moon Rhea. *Science* 330: 1813–1815.
Tokar RL, Johnson RE, Thomson MF, et al. (2012) Detection of O_2^+ at Saturn's moon Dione. *Geophysical Research Letters* 39: L03105.
Valentine DL (2002) Biogeochemistry and microbial ecology of methane oxidation in anoxic environments: A review. *Antonie Van Leeuwenhoek International Journal of General and Molecular Microbiology* 81: 271–282.
Waldbauer JR, Sherman LS, Sumner DY, and Summons RE (2009) Late Archean molecular fossils from the Transvaal Supergroup record the antiquity of microbial diversity and aerobiosis. *Precambrian Research* 169: 28–47.
Walker JCG (1977) *Evolution of the Atmosphere*. New York: Macmillan.
Warneck P (2000) *Chemistry of the Natural Atmosphere*, 927p. New York: Academic.
Watson AJ, Donahue TM, and Kuhn WR (1984) Temperatures in a runaway greenhouse on the evolving Venus: Implications for water-loss. *Earth and Planetary Science Letters* 68: 1–6.
Wedepohl KH (1995) The composition of the continental crust. *Geochimica et Cosmochimica Acta* 59: 1217–1232.
Wille M, Kramers JD, Nagler TF, et al. (2007) Evidence for a gradual rise of oxygen between 2.6 and 2.5 Ga from Mo isotopes and Re-PGE signatures in shales. *Geochimica et Cosmochimica Acta* 71: 2417–2435.
Williford KH, Van Kranendonk MJ, Ushikubo T, Kozdon R, and Valley JW (2011) Constraining atmospheric oxygen and seawater sulfate concentrations during Paleoproterozoic glaciation: In situ sulfur three-isotope microanalysis of pyrite from the Turee Creek Group, Western Australia. *Geochimica et Cosmochimica Acta* 75: 5686–5705.
Xiong J (2006) Photosynthesis: What color was its origin? *Genome Biology* 7: 245.
Zahnle K, Claire M, and Catling D (2006) The loss of mass-independent fractionation in sulfur due to a Paleoproterozoic collapse of atmospheric methane. *Geobiology* 4: 271–283.
Zahnle KJ and Kasting JF (1986) Mass fractionation during transonic escape and implications for loss of water from Mars and Venus. *Icarus* 68: 462–480.
Zahnle KJ and Sleep NH (2002) Carbon dioxide cycling through the mantle and its implications for the climate of the ancient Earth. *Geological Society of London Special Publication* 199: 231–257.